2

IMAGING TECHNIQUES (MICROSCOPY)

2.0 INTRODUCTION

The four techniques included in this chapter all have microscopy in their names. Their role (but certainly not only their only one) is to provide a magnified image. The objective, at its simplest, is to observe features that are beyond the resolution of the human eye (about 100 μm). Since the eye uses visible wavelength light, only a Light Microscope can do this directly. Reflected or transmitted light from the sample enters the eye after passing through a magnification column. All other microscopy imaging techniques use some other interaction probe and response signal (usually electrons) to provide the *contrast* that produces an image. The response signal image, or map, is then processed in some way to provide an optical equivalent "picture" for us to see. We usually think of images as three dimensional, with the object as "solid." The microscopies have different capabilities, not only in terms of magnification and lateral resolution, but also in their ability to represent *depth*. In the light microscope, topological contrast is provided largely by shadowing in reflection. In Scanning Electron Microscopy, SEM, the topological contrast is there because the efficiency of generating secondary electrons (the signal), which originate from the several top tens of nanometers of material, strongly depends on the angle at which the probe beam strikes the surface. In Scanning Tunneling Microscopy/Scanning Force Microscopy, STM/SFM, the surface is directly profiled by scanning a tip, capable of following topology at atomic-scale resolution,

across the surface. In Transmission Electron Microscopy, TEM, which can also achieve atomic-scale *lateral* resolution, *no* depth information is obtained because the technique works by having the probe electron beam transmitted through a sample that is up to 200 nm thick.

If one wants only to better identify regions for further examination by other techniques, the Light Microscope is likely to be the first imaging instrument used. Around for over 150 years, it is capable of handling every type of sample (though different types of microscope are better suited to differing applications), and can easily provide magnification up to 1400×, the useful limit for visible wavelengths. By utilizing polarizers, many other properties, in addition to size and shape, become accessible (e. g., refractive index, crystal system, melting point, etc.). There are enormous collections of data (atlases) to help the observer identify what he or she is seeing and to interpret it. Light microscopes are also the cheapest "modern" instrument and take up the least physical space.

The next instrument likely to be used is the SEM where magnified images of up to 300k× are obtainable, the wavelength of electrons not being nearly so limiting as that of visible light, and lateral features down to a few nm become resolvable. Sample requirements are more stringent, however. They must be vacuum compatible, and must be either conducting or coated with a thin conducting layer. A variety of contrast mechanisms exist, in addition to the topological, enabling the production of maps distinguishing high- and low-Z elements, defects, magnetic domains, and even electrically charged regions in semiconductors. The *depth* from which all this information comes varies from nanometers to micrometers, depending on the primary beam energy used and the particular physical process providing the contrast. Likewise, the lateral resolution in these analytical modes also varies and is always poorer than the topological contrast mode. The cost and size range are about a factor of 5 to 10 greater than for light microscopes.

STMs and SFMs are a new breed of instrument invented in 1981 and 1985, respectively. Their enormous lateral resolution capability (atomic for STM; a little lower for SFM) and vertical resolution capability (0.01 Å for STM, 0.1 Å for SFM) come about because the interactions involved between the scanning tip and the surface are such as to be limited to a few atoms on the tip (down to one) and a few atoms on the surface. Though famous for their use in imaging single atoms or molecules, and moving them under control on clean surfaces in pristine UHV conditions, their practical uses in ambient atmosphere, including liquids, to profile large areas at reduced resolution have gained rapid acceptance in applied science and engineering. Features on the nanometer scale, sometimes not easily seen in SEM, can be observed in STM/SFM. There are however no ancillary analytical modes, such as in SEM. Costs are in the same range as SEMs. Space requirements are reduced.

The final technique in this chapter, TEM, has been a mainstay of materials science for 30 years. It has become ever more powerful, specialized, and expensive. A

well-equipped TEM laboratory today has 2 or 3 TEMs with widely different capabilities and the highest resolution/highest electron energy TEMs probably cost over $1 million. Sample preparation in TEM is *critical*, since the sample sizes accepted are usually less than 3 mm in diameter and 200 nm in thickness (so that the electron beam can pass through the sample). This distinguishes TEM from the other techniques for which very little preparation is needed. It is quite common for excellent TEMs to stand idle or fail in their tasks because of inadequacy in the ancillary sample preparation equipment or the lack of qualified manpower there. A complex variety of operation modes exist in TEM, all either variations or combinations of *imaging* and *diffraction* methods. Switching from one mode to another in modern instruments is trivial, but interpretation is *not* trivial for the nonspecialist. The combination of imaging (with lateral magnification up to 1M×) with a variety of contrast modes, plus an atomic resolution mode for crystalline material (phase contrast in HREM), together with small and large area diffraction modes, provide a wealth of characterization information for the expert. This is always summed through a column of atoms (maybe 100), however, with *no* depth information included. Clearly then, TEM is a thin-film technique rather than a surface or interface technique, unless interfaces are viewed in cross section.

2.1 Light Microscopy

JOHN GUSTAV DELLY

Contents

Introduction

The practice of light microscopy goes back about 300 years. The light microscope is a deceptively simple instrument, being essentially an extension of our own eyes. It magnifies small objects, enabling us to directly view structures that are below the resolving power of the human eye (0.1 mm). There is as much difference between materials at the microscopic level as there is at the macroscopic level, and the practice of microscopy involves learning the microscopic characteristics of materials. These direct visual methods were applied first to plants and animals, and then, in the mid 1800s, to inorganic forms, such as thin sections of rocks and minerals, and polished metal specimens. Since then, the light microscope has been used to view virtually all materials, regardless of nature or origin.

Basic Principles

In the biomedical fields, the ability of the microscopist is limited only by his or her capacity to remember the thousands of distinguishing characteristics of various tissues; as an aid, atlases of tissue structures have been prepared over the years. Like-

wise, in materials characterization, atlases and textbooks have been prepared to aid the analytical microscopist. In addition, the analytical microscopist typically has a collection of reference standards for direct comparison to the sample under study. Atlases may be specific to a narrow subfield, or may be quite general and universal. There are microscopical atlases for the identification of metals and alloys,[1] rocks and ores,[2] paper fibers, animal feeds, pollens, foods, woods, animal hairs, synthetic fibers, vegetable drugs, and insect fragments, as well as universal atlases that include everything, regardless of nature or origin,[3, 4] and, finally, atlases of the latest composites.

The familiar light microscope used by biomedical scientists is not suitable for the study of materials. Biomedical workers rely almost solely on morphological characteristics of cells and tissues. In the materials sciences, too many things look alike; however, their structures may be quite different internally and, if crystalline, quite specific. Ordinary white light cannot be used to study such materials principally because the light vibrates in all directions and consists of a range of wavelengths, resulting in a composite of information—which is analytically useless. The instrument of choice for the study of materials is the polarized light microscope. By placing a polarizer in the light's path before the sample, light is made to vibrate in one direction only, which enables the microscopist to isolate specific properties of materials in specific orientations. For example, with ordinary white light, one can determine only morphology (shape) and size; if a polarizer is added, the additional properties of pleochroism (change in color or hue relative to orientation of polarized light) and refractive indices may be determined. By the addition of a second polarizer above the specimen, still other properties may be determined; namely, birefringence (the numerical difference between the principal refractive indices), the sign of elongation (location of the high and low refractive indices in an elongated specimen), and the extinction angle (the angle between the vibration direction of light inside the specimen and some prominent crystal face). Some of these may be determined by simply adding polarizers to an ordinary microscope, but true, quantitative polarized light microscopy and conoscopy (observations and measurements made at the objective back focal plane) can be performed only by using polarizing microscopes with their many graduated adjustments.

Some of the characteristics of materials that may be determined with the polarized light microscope include

- Morphology
- Size
- Transparency or opacity
- Color (reflected and transmitted)
- Refractive indices
- Dispersion of refractive indices

- Pleochroism
- Dispersion staining colors
- Crystal system
- Birefringence
- Sign of elongation
- Optic sign
- Extinction angle
- Fluorescence (ultraviolet, visible, and infrared)
- Melting point
- Polymorphism
- Eutectics
- Degree of crystallinity
- Microhardness.

The modern light microscope is constructed in modular form, and may be configured in many ways depending on the kind of material that is being studied. Transparent materials, whether wholly or partly so, are studied with transmitted light; opaque specimens are studied with an episystem (reflected light; incident light), in which the specimen is illuminated from above. Materials scientists who study all kinds of materials use so-called "universal" microscopes, which may be converted quickly from one kind to another.

Sample Preparation

Sample preparation methods vary widely. The very first procedure for characterizing any material simply is to look at it using a low-power stereomicroscope; often, a material can be characterized or a problem solved at this stage. If examination at this level does not produce an answer, it usually suggests what needs to be done next: go to higher magnification; mount for FTIR, XRD, or EDS; section; isolate contaminants; and so forth.

If the material is particulate, it needs to be mounted in a refractive index liquid for determination of its optical properties. If the sample is a metal, or some other hard material, it may need to be embedded in a polymer matrix and then sawn, ground, polished, and etched[5] before viewing. Polymers may be viewed directly, but usually need to be sectioned. This may involve embedding the sample to support the material and prevent preparation artifacts. Sectioning may be done dry and at room temperature using a hand, rotary, rocking, or sledge microtome (a large bench microtome incorporating a knife that slides horizontally), or it may need to be done at freezing temperatures with a cryomicrotome, which uses glass knives.

If elemental or compound data are required, the material needs to be mounted for the appropriate analytical instrument. For example, if light microscopy shows a

sample to be a metal it can be put into solution and its elemental composition determined by classical microchemical tests; in well-equipped microscopy laboratories, some sort of microprobe (for example, electron- or ion-microprobe) is usually available, and as these are nondestructive by comparison, the sample is mounted for them using the low-power stereomicroscope. Individual samples <1 μm are handled freehand by experienced particle handlers under cleanroom conditions. A particle may be mounted on a beryllium substrate for examination by an electron microprobe, using a minimal amount of flexible collodion as an adhesive, or it may be mounted on an aluminum stub for SEM, on the end of a glass fiber for micro-XRD, or on a thin cleavage fragment of sodium chloride ("salt plate") for micro-FTIR. The exact procedures for preparing the instruments and mounting particles for various analyses have been described in detail.[4]

Detection Limits

Many kinds of materials, because of their color by transmitted light and their optical properties, can be detected even when present in sizes below the instrument's resolving power, but cannot be analyzed with confidence. Organized structures like diatom fragments can be identified on sight, even when very small, but an unoriented polymer cannot be characterized by morphology alone. The numerical aperture, which is engraved on each objective and condenser, is a measure of the light-gathering ability of the objective, or light-providing ability of the condenser. Specifically, the numerical aperture *NA* is defined as

$$NA = n\sin\frac{AA}{2} \tag{1}$$

where n is the refractive index of the medium between the cover glass and the objective front lens, and *AA* is the angular aperture of the objective. The maximum theoretical *NA* of a dry system is 1.0; the practical maximum is 0.95. Higher values of *NA* can be obtained only by using oil-immersion objectives and condensers.The oils used for this have a refractive index of 1.515; the practical maximum numerical aperture achieved is 1.4. The significance of the numerical aperture lies in the diffraction theory of microscopical image formation; details on the theoretical and practical limits of the light microscope are readily available.[6]

The theoretical limit to an instrument's resolving power is determined by the wavelength of light used, and the numerical aperture of the system:

$$r = \frac{\lambda}{2NA} \tag{2}$$

where r is the resolving power, λ is the wavelength of light used, and *NA* is the numerical aperture of the system. The wavelength is taken to be 0.55 μm when using white light. The use of ultraviolet microscopy effectively doubles the resolving power, but the lenses must be made of quartz and photographic methods or

image converter tubes must be used to image the specimen. The maximum theoretical limit of resolving power is currently about 0.2 μm, using white light and conventional light microscopes. The practical limit to the maximum useful magnification, *MUM*, is 1000 *NA*. In modern microscopes *MUM* = 1400×. Although many instruments easily provide magnifications of 2000–5000×, this is "empty" magnification; i.e., no more detail is revealed beyond that seen at 1400×.

Common Modes of Analysis

Particulate materials are usually analyzed with a polarizing microscope set up for transmitted light. This allows one to determine the shape, size, color, pleochroism, refractive indices, birefringence, sign of elongation, extinction angle, optic sign, and crystal system, to name but a few characteristics. If the sample is colorless, transparent, and isotropic, and is embedded in a matrix with similar properties, it will not be seen, or will be seen only with difficulty, because our eyes are sensitive to amplitude and wavelength differences, but not to phase differences. In this case, the mode must be changed to phase contrast. This technique, introduced by Zernike in the 1930s, converts phase differences into amplitude differences. Normarski differential interference contrast is another mode that may be set up. Both modes are qualitative methods of increasing contrast. Quantitative methods are available via interference microscopy.

Darkfield microscopy is one of the oldest modes of microscopy. Here, axial rays from the condenser are prevented from entering the objective, through the use of an opaque stop placed in the condenser, while peripheral light illuminates the specimen. Thus, the specimen is seen lighted against a dark field.

For studying settled materials in liquids, or for very large opaque specimens, the inverted microscope may be used.

For fluorescence microscopy the light source is changed from an incandescent lamp to a high-pressure mercury vapor burner, which is rich in wavelengths below the visible. Exciter filters placed in the light path isolate various parts of the spectrum. The 365-nm wavelength is commonly used in fluorescence microscopy to characterize a material's primary fluorescence, or to detect a tracer fluorochrome through secondary fluorescence. The 400-nm wavelength region is another commonly used exciter.

Attachment of a hot or cold stage to the ordinary microscope stage allows the specimen to be observed while the temperature is changed slowly, rapidly, or held constant somewhere other than ambient. This technique is used to determine melting and freezing points, but is especially useful for the study of polymorphs, the determination of eutectics, and the preparation of phase diagrams.

Spindle stages and universal stages allow a sample to be placed in any orientation relative to the microscope's optical axis.

Not every sample requires all modes for complete characterization; most samples yield to a few procedures. Let us take as an example some particulate material—this

may be a sample of lunar dust fines, a contaminant removed from a failed integrated circuit, a new pharmaceutical or explosive, a corrosion product or wear particle, a fiber from a crime scene, or a pigment from an oil painting—the procedure will be the same. A bit of the sample, or a single particle, is placed on a microscope slide in a suitable mounting medium, and a cover slip is placed on top. The mounting medium is selected from a series of refractive index liquid standards which range from about 1.300 to 1.800—usually something around 1.660 is selected because it provides good contrast with a wide variety of industrial materials. The sample is then placed on the stage of the polarizing microscope and brought into focus. At this point the microscope may be set up for plane-polarized light or slightly uncrossed polarizers—the latter is more useful. Several characteristics will be immediately apparent: the morphology, relative size, and isotropy or anisotropy. If the sample cannot be seen at any orientation between fully crossed polarizers, it is isotropic; it has only one refractive index, and is either amorphous or in the cubic crystal system. If it can be seen, it will display one or more colors in the Newtonian series; this indicates that it has more than one refractive index, or, if it is only spotty, that it has some kind of strain birefringence or internal orientation.

The analyzer is removed and the color of the sample is observed in plane-polarized light. If the sample is colored, the stage is rotated. Colored, anisotropic materials may show pleochroism—a change in color or hue when the orientation with respect to the vibration direction of the polarizer is changed. Any pleochroism should be noted and recorded.

Introducing a monochromatic filter—usually 589 nm—and closing the aperture diaphragm while using a high numerical aperture objective, the focus is changed from best focus position to above best focus. The diffraction halo seen around the particle (Becke line) will move into or away from the particle, thus indicating the relative refractive index. By orienting the specimen and rotating the stage, more than one refractive index may be noted.

With polarizers fully crossed and the specimen rotated to maximum brightness, the sample thickness is determined with the aid of a calibrated eyepiece micrometer, and the polarization (retardation) color is noted. From these the birefringence may be determined mathematically or graphically with the aid of a Michel-Lévy chart.

If the sample is elongated, it is oriented 2 o'clock–8 o'clock, the retardation color is noted, and a compensator is inserted in the slot above the specimen. The retardation colors will go upscale or downscale; i.e., they will be additive or subtractive. This will indicate where the high and low refractive indices are located with respect to the long axis of the sample. This is the sign of elongation, and is said to be positive if the sample is "length slow" (high refractive index parallel to length), or negative if the sample is "length fast" (low refractive index parallel to length).

The elongated sample is next rotated parallel to an eyepiece crosshair, and one notes if the sample goes to extinction; if it does, it has parallel extinction (the vibra-

Figure 1 **Nikon Optiphot-2 polarizing microscope.**

tional directions inside the sample are parallel to the vibrational directions of the polarizer and analyzer). If the sample does not go to extinction, the stage reading is noted and the sample is rotated to extinction (not greater than 45°); the stage reading is again noted, and the difference between the readings is the extinction angle.

If necessary, each refractive index is determined specifically through successive immersion in liquids of various refractive index until one is found where the sample disappears—knowing the refractive index of the liquid, one then knows the refractive index in a particular orientation. There may be one, two, or three principal refractive indices.

The Bertrand lens, an auxiliary lens that is focused on the objective back focal plane, is inserted with the sample between fully crossed polarizers, and the sample is oriented to show the lowest retardation colors. This will yield interference figures, which immediately reveal whether the sample is uniaxial (hexagonal or tetragonal) or biaxial (orthorhombic, monoclinic, or triclinic). Addition of the compensator and proper orientation of the rotating stage will further reveal whether the sample is optically positive or negative.

These operations are performed faster than it takes to describe them, and are usually sufficient to characterize a material. The specific steps to perform each of the above may be found in any textbook on optical crystallography.

Sample Requirements

There are no specific sample requirements; all samples are accommodated.

Figure 2 **Nikon Epithot inverted metallograph.**

Artifacts

Artifacts may be introduced from the environment or through preparative techniques. When assessing individual tiny particles of material, the risk of loss or contamination is high, so that samples of this nature are handled and prepared for examination in a clean bench or a cleanroom (class 100 or better).

Artifacts introduced through sample preparation are common materials; these may be bits of facial tissue, wax, epithelial cells, hair, or dried stain, all inadvertently introduced by the microscopist. Detergent residues on so-called "precleaned" microscope slides and broken glass are common artifacts, as are knife marks and chatter marks from sectioning with a faulty blade, or scratch marks from grinding and polishing.

Quantification

For other quantification, specialized graticules are available, including point counting, grids, concentric circles, and special scales. The latest methods of quantification involve automatic image analysis.

Instrumentation

Figure 1 illustrates a typical, good quality, analytical polarizing microscope. Polarizing microscopes are extraordinarily versatile instruments that enable the trained microscopist to characterize materials rapidly and accurately.

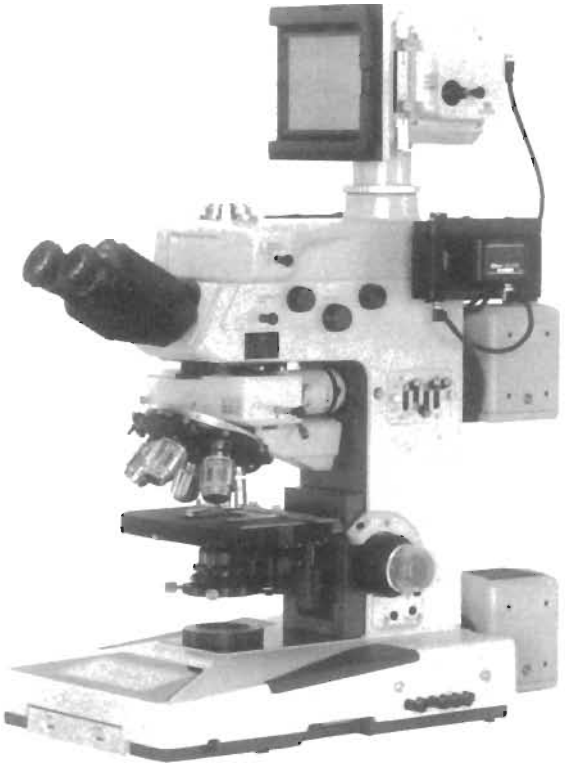

Figure 3 **Nikon Microphot-FXA research microscope for materials science.**

As an example of a more specific application, Figure 2 illustrates a metallograph—a light microscope set up for the characterization of opaque samples. Figure 3 illustrates a research-grade microscope made specifically for materials science, i.e., for optically characterizing all transparent and translucent materials.

Conclusions

The classical polarizing light microscope as developed 150 years ago is still the most versatile, least expensive analytical instrument in the hands of an experienced microscopist. Its limitations in terms of resolving power, depth of field, and contrast have been reduced in the last decade, in which we have witnessed a revolution in its evolution. Video microscopy has increased contrast electronically, and thereby revealed structures never before seen. With computer enhancement, unheard of resolutions are possible. There are daily developments in the X-ray, holographic, acoustic, confocal laser scanning, and scanning tunneling microscopes.[7, 8]

The general utility of the light microscope is also recognized by its incorporation into so many other kinds of analytical instrumentation. Continued development of new composites and materials, together with continued trends in microminiaturization make the simple, classical polarized-light microscope the instrument of choice for any initial analytical duty.

Related Articles in the Encyclopedia

None in this volume.

References

1 ASM Handbook Committee. *Metals Handbook, Volume 7: Atlas of Microstructures.* American Society of Metals, Metals Park, 1972.

2 O. Oelsner. *Atlas of the Most Important Ore Mineral Parageneses Under the Microscope.* Pergamon, London, 1961 (English edition, 1966).

3 A. A. Benedetti-Pichler. *Identification of Materials.* Springer-Verlag, New York, 1964.

4 W. C. McCrone, and J. G. Delly. *The Particle Atlas.* Ann Arbor Science, Ann Arbor, 1973, Volumes 1–4; and S. Palenik., 1979, Volume 5; and J. A. Brown and I. M. Stewart, 1980, Volume 6.

5 G. L. Kehl. *The Principles of Metallographic Laboratory Practice.* McGraw-Hill, New York, 1949.

6 J. G. Delly. *Photography Through The Microscope.* Eastman Kodak Company, Rochester, 1988.

7 *Modern Microscopies.* (P. J. Duke and A. G. Michette, eds.) Plenum, New York, 1990.

8 M. Pluta. *Advanced Light Microscopy.* Elsevier, Amsterdam, 1988.

2.2 SEM

Scanning Electron Microscopy

JEFFREY B. BINDELL

Contents

Introduction

Traditionally, the first instrument that would come to mind for small scale materials characterization would be the optical microscope. The optical microscope offered the scientist a first look at most samples and could be used to routinely document the progress of an investigation. As the sophistication of investigations increased, the optical microscope often has been replaced by instrumentation having superior spatial resolution or depth of focus. However, its use has continued because of the ubiquitous availability of the tool.

For the purpose of a detailed materials characterization, the optical microscope has been supplanted by two more potent instruments: the Transmission Electron Microscope (TEM) and the Scanning Electron Microscope (SEM). Because of its reasonable cost and the wide range of information that it provides in a timely manner, the SEM often replaces the optical microscope as the preferred starting tool for materials studies.

The SEM provides the investigator with a highly magnified image of the surface of a material that is very similar to what one would expect if one could actually "see" the surface visually. This tends to simplify image interpretations considerably, but

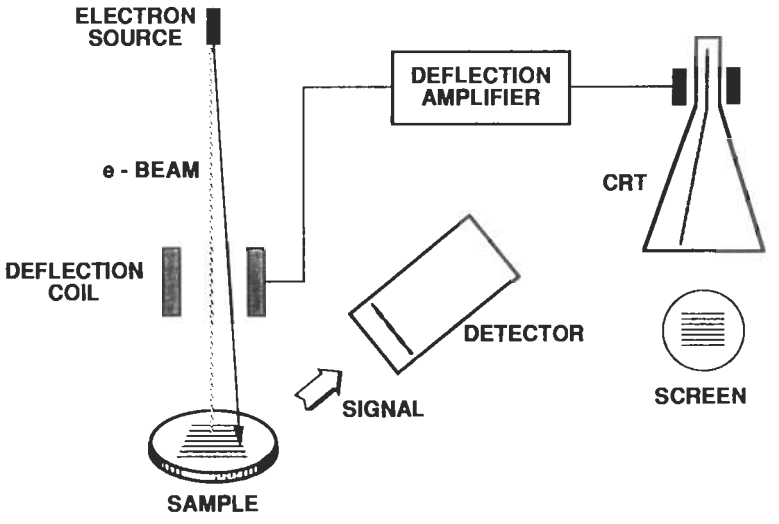

Figure 1 **Schematic describing the operation of an SEM.**

reliance on intuitive reactions to SEM images can, on occasion, lead to erroneous results. The resolution of the SEM can approach a few nm and it can operate at magnifications that are easily adjusted from about 10×–300,000×.

Not only is topographical information produced in the SEM, but information concerning the composition near surface regions of the material is provided as well. There are also a number of important instruments closely related to the SEM, notably the electron microprobe (EMP) and the scanning Auger microprobe (SAM). Both of these instruments, as well as the TEM, are described in detail elsewhere in this volume.

Physical Basis of Operation

In the SEM, a source of electrons is focused (in vacuum) into a fine probe that is rastered over the surface of the specimen, Figure 1. As the electrons penetrate the surface, a number of interactions occur that can result in the emission of electrons or photons from (or through) the surface. A reasonable fraction of the electrons emitted can be collected by appropriate detectors, and the output can be used to modulate the brightness of a cathode ray tube (CRT) whose x- and y-inputs are driven in synchronism with the x–y voltages rastering the electron beam. In this way an image is produced on the CRT; every point that the beam strikes on the sample is mapped directly onto a corresponding point on the screen. If the amplitude of the saw-tooth voltage applied to the x- and y-deflection amplifiers in the SEM is reduced by some factor while the CRT saw-tooth voltage is kept fixed at the level

necessary to produce a full screen display, the magnification, as viewed on the screen, will be increased by the same factor.

The principle images produced in the SEM are of three types: secondary electron images, backscattered electron images, and elemental X-ray maps. Secondary and backscattered electrons are conventionally separated according to their energies. They are produced by different mechanisms. When a high-energy primary electron interacts with an atom, it undergoes either inelastic scattering with atomic electrons or elastic scattering with the atomic nucleus. In an inelastic collision with an electron, some amount of energy is transferred to the other electron. If the energy transfer is very small, the emitted electron will probably not have enough energy to exit the surface. If the energy transferred exceeds the work function of the material, the emitted electron can exit the solid. When the energy of the emitted electron is less than about 50 eV, by convention it is referred to as a secondary electron (SE), or simply a *secondary*. Most of the emitted secondaries are produced within the first few nm of the surface. Secondaries produced much deeper in the material suffer additional inelastic collisions, which lower their energy and trap them in the interior of the solid.

Higher energy electrons are primary electrons that have been scattered without loss of kinetic energy (i.e., elastically) by the nucleus of an atom, although these collisions may occur after the primary electron has already lost some of its energy to inelastic scattering. Backscattered electrons (BSEs) are considered to be the electrons that exit the specimen with an energy greater then 50 eV, including Auger electrons. However most BSEs have energies comparable to the energy of the primary beam. The higher the atomic number of a material, the more likely it is that backscattering will occur. Thus as a beam passes from a low-Z (atomic number) to a high-Z area, the signal due to backscattering, and consequently the image brightness, will increase. There is a built in contrast caused by elemental differences.

One further breaks down the secondary electron contributions into three groups: SEI, SEII and SEIII. SEIs result from the interaction of the incident beam with the sample at the point of entry. SEIIs are produced by BSE s on exiting the sample. SEIIIs are produced by BSEs which have exited the surface of the sample and further interact with components on the interior of the SEM usually not related to the sample. SEIIs and SEIIIs come from regions far outside that defined by the incident probe and can cause serious degradation of the resolution of the image.

It is usual to define the primary beam current i_0, the BSE current i_{BSE}, the SE current i_{SE}, and the sample current transmitted through the specimen to ground i_{SC}, such that the Kirchoff current law holds:

$$i_0 = i_{BSE} + i_{SE} + i_{SC} \tag{1}$$

These signals can be used to form complementary images. As the beam current is increased, each of these currents will also increase. The backscattered electron yield η and the secondary electron yield δ, which refer to the number of backscattered and secondary electrons emitted per incident electron, respectively, are defined by the relationships:

$$\eta = \frac{i_{BSE}}{i_0} \tag{2}$$

$$\delta = \frac{i_{SE}}{i_0} \tag{3}$$

In most currently available SEMs, the energy of the primary electron beam can range from a few hundred eV up to 30 keV. The values of δ and η will change over this range, however, yielding micrographs that may vary in appearance and information content as the energy of the primary beam is changed. The value of the BSE yield increases with atomic number Z, but its value for a fixed Z remains constant for all beam energies above 5 keV. The SE yield δ decreases slowly with increasing beam energy after reaching a peak at some low voltage, usually around 1 keV. For any fixed voltage, however, δ shows very little variation over the full range of Z. Both the secondary and backscattered electron yields increase with decreasing glancing angle of incidence because more scattering occurs closer to the surface. This is one of the major reasons why the SEM provides excellent topographical contrast in the SE mode; as the surface changes its slope, the number of secondary electrons produced changes as well. With the BSEs this effect is not as prominent, since to fully realize it the BSE detector would have to be repositioned to measure forward scattering.

An additional electron interaction of major importance in the SEM occurs when the primary electron collides with and ejects a core electron from an atom in the solid. The excited atom will decay to its ground state by emitting either a characteristic X-ray photon or an Auger electron (see the article on AES). The X-ray emission signal can be sorted by energy in an energy dispersive X-ray detector (see the article on EDS) or by wavelength with a wavelength spectrometer (see the article on EPMA). These distributions are characteristic of the elements that produced them and the SEM can use these signals to produce elemental images that show the spatial distribution of particular elements in the field of view. The primary electrons can travel considerable distances into a solid before losing enough energy through collisions to be no longer able to excite X-ray emission. This means that a large volume of the sample will produce X-ray emission for any position of the smaller primary beam, and consequently the spatial resolution of this type of image will rarely be better than 0.5 μm.

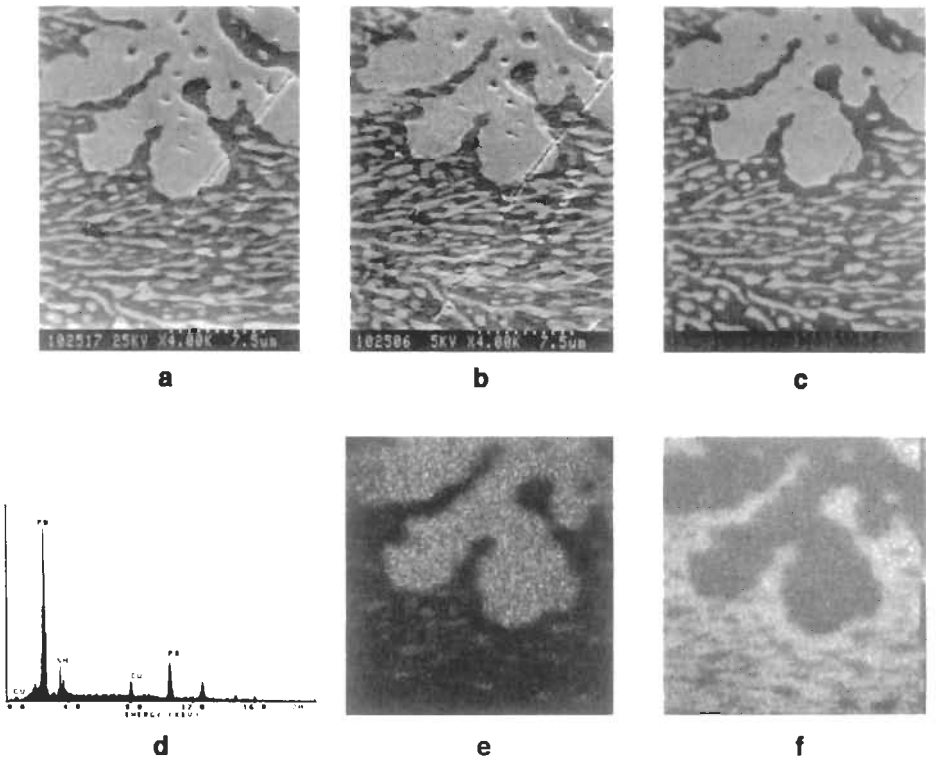

Figure 2 **Micrographs of the same region of a specimen in various imaging modes on a high-resolution SEM: (a) and (b) SE micrographs taken at 25 and 5 keV, respectively; (c) backscattered image taken at 25 keV; (d) EDS spectrum taken from the Pb-rich phase of the Pb-Sn solder; (e) and (f) elemental maps of the two elements taken by accepting only signals from the appropriate spectral energy regions.**

An illustration of this discussion can be seen in Figure 2, which is a collection of SEM images taken from the surface of a Pb-Sn solder sample contaminated with a low concentration of Cu. Figure 1a, a secondary electron image (SE) taken with a primary energy of 25 keV, distinguishes the two Pb-Sn eutectic phases as brighter regions (almost pure Pb) separated by darker bands corresponding to the Sn-rich phase. The micrograph originally was taken at a magnification of 4000× but care should be exercised when viewing published examples because of the likelihood of photographic enlargement or reduction by the printer. Most SEMs produce a marker directly on the photograph that defines the actual magnification. In the present example, the series of dots at the bottom of the micrograph span a physical distance of 7.5 μm. This can be used as an internally consistent ruler for measurement purposes.

The micrograph also shows the presence of a scratch that goes diagonally across the entire field of view. Note the appearance of depth to this scratch as a result of the variation in secondary electron yield with the local slope of the surface. The spatial resolution of the SEM due to SEIs usually improves with increasing energy of the primary beam because the beam can be focused into a smaller spot. Conversely, at higher energies the increased penetration of the electron beam into the sample will increase the interaction volume, which may cause some degradation of the image resolution due to SEIIs and SEIIIs. This is shown in Figure 2b, which is a SE image taken at only 5 keV. In this case the reduced electron penetration brings out more surface detail in the micrograph.

There are two ways to produce a backscattered electron image. One is to put a grid between the sample and the SE detector with a –50-V bias applied to it. This will repel the SEs since only the BSEs will have sufficient energy to penetrate the electric field of the grid. This type of detector is not very effective for the detection of BSEs because of its small solid angle of collection. A much larger solid angle of collection is obtained by placing the detector immediately above the sample to collect the BSE. Two types of detectors are commonly used here. One type uses partially depleted n-type silicon diodes coated with a layer of gold, which convert the incident BSEs into electron–hole pairs at the rate of 1 pair per 3.8 eV. Using a pair of Si detectors makes it possible to separate atomic number contrast from topographical contrast. The other detector type, the so-called scintillator photo multiplier detector, uses a material that will fluoresce under the bombardment of the high-energy BSEs to produce a light signal that can be further amplified. The photomultiplier detector was used to produce the BSE micrograph in Figure 2c. Since no secondary electrons are present, the surface topography of the scratch is no longer evident and only atomic number contrast appears.

Atomic number contrast can be used to estimate concentrations in binary alloys because the actual BSE signal increases somewhat predictably with the concentration of the heavier element of the pair.

Both energy-dispersive and wavelength-dispersive X-ray detectors can be used for elemental detection in the SEM. The detectors produce an output signal that is proportional to the number of X-ray photons in the area under electron bombardment. With an EDS the output is displayed as a histogram of counts versus X-ray energy. Such a display is shown in Figure 2d. This spectrum was produced by allowing the electron beam to dwell on one of the Pb-rich areas of the sample. The spectrum shows the presence of peaks corresponding to Pb and a small amount of Sn. Since this sample was slightly contaminated with Cu, the small Cu peak at 8 keV is expected. The detectors can be adjusted to pass only a range of pulses corresponding to a single X-ray spectral peak that is characteristic of a particular element. This output can then be used to produce an elemental image or an X-ray map; two X-ray maps using an EDS are shown in Figure 2e for Pb and in Figure 2f for Sn. Note the complementary nature of these images, and how easy it is to iden-

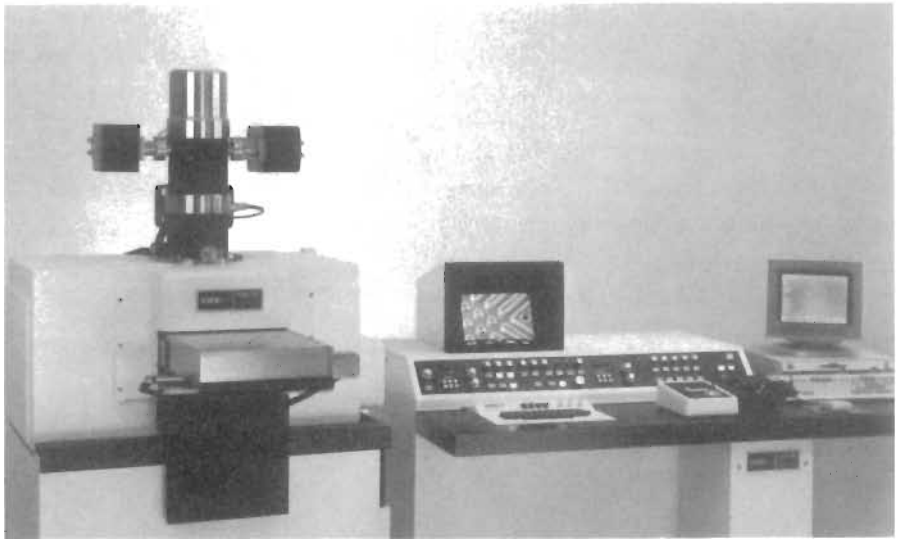

Figure 3 **Photograph of a modern field emission SEM. (Courtesy of AMRAY Inc., Bedford, MA)**

tify portions of the SE or BSE image having specific local compositions. The data usually can be quantified through the use of appropriate elemental standards and well-established computational algorithms.

Instrumentation

Figure 3 shows a photograph of a recent model SEM. The main features of the instrument are the electron column containing the electron source (i.e., the gun), the magnetic focusing lenses, the sample vacuum chamber and stage region (at the bottom of the column) and the electronics console containing the control panel, the electronic power supplies and the scanning modules. A solid state EDS X-ray detector is usually attached to the column and protrudes into the area immediately above the stage; the electronics for the detector are in separate modules, but there has been a recent trend toward integration into the SEM system architecture.

The overall function of the electron gun is to produce a source of electrons emanating from as small a "spot" as possible. The lenses act to demagnify this spot and focus it onto a sample. The gun itself produces electron emission from a small area and then demagnifies it initially before presenting it to the lens stack. The actual emission area might be a few μm in diameter and will be focused eventually into a spot as small as 1 or 2 nm on the specimen.

There are three major types of electron sources: thermionic tungsten, LaB_6, and hot and cold field emission. In the first case, a tungsten filament is heated to allow

electrons to be emitted via thermionic emission. Temperatures as high as 3000° C are required to produce a sufficiently bright source. These filaments are easy to work with but have to be replaced frequently because of evaporation. The material LaB_6 has a lower work function than tungsten and thus can be operated at lower temperatures, and it yields a higher source brightness. However, LaB_6 filaments require a much better vacuum then tungsten to achieve good stability and a longer lifetime. The brighter the source, the higher the current density in the spot, which consequently permits more electrons to be focused onto the same area of a specimen. Recently, field emission electron sources have been produced. These tips are very sharp; the strong electric field created at the tip extracts electrons from the source even at low temperatures. Emission can be increased by thermal assistance but the energy width of the emitted electrons may increase somewhat. The sharper the energy profile, the less the effect of chromatic aberrations of the magnetic defocusing lenses. Although they are more difficult to work with, require very high vacuum and occasional cleaning and sharpening via thermal flashing, the enhanced resolution and low voltage applications of field emission tips are making them the source of choice in newer instruments that have the high-vacuum capability necessary to support them.

The beam is defocused by a series of magnetic lenses as shown in Figure 4. Each lens has an associated defining aperture that limits the divergence of the electron beam. The top lenses are called *condenser* lenses, and often are operated as if they were a single lens. By increasing the current through the condenser lens, the focal length is decreased and the divergence increases. The lens therefore passes less beam current on to the next lens in the chain. Increasing the current through the first lens reduces the size of the image produced (thus the term spot size for this control). It also spreads out the beam resulting in beam current control as well. Smaller spot sizes, often given higher dial numbers to correspond with the higher lens currents required for better resolution, are attained with less current (signal) and a smaller signal-to-noise ratio. Very high magnification images therefore are inherently noisy.

The beam next arrives at the final lens–aperture combination. The final lens does the ultimate focusing of the beam onto the surface of the sample. The sample is attached to a specimen stage that provides x- and y-motion, as well as tilt with respect to the beam axis and rotation about an axis normal to the specimen's surface. A final "z" motion allows for adjustment of the distance between the final lens and the sample's surface. This distance is called the *working distance.*

The working distance and the limiting aperture size determine the convergence angle shown in the figure. Typically the convergence angle is a few mrad and it can be decreased by using a smaller final aperture or by increasing the working distance. The smaller the convergence angle, the more variation in the z-direction topography that can be tolerated while still remaining in focus to some prescribed degree. This large depth of focus contributes to the ease of observation of topographical

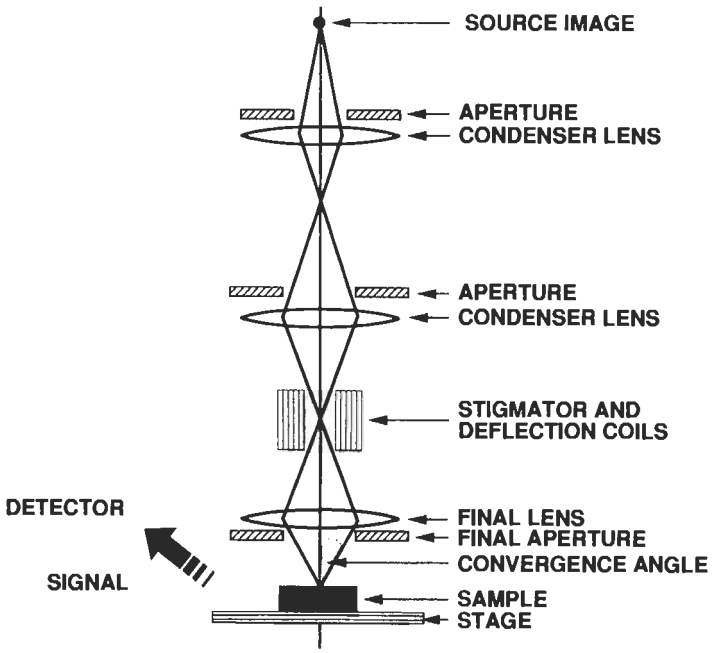

Figure 4 **Schematic of the electron optics constituting the SEM.**

effects. The depth of focus in the SEM is compared in Figure 5 with that of an optical microscope operated at the same magnification for viewing the top of a common machine screw.

Sample Requirements

The use of the SEM requires very little in regard to sample preparation, provided that the specimen is vacuum compatible. If the sample is conducting, the major limitation is whether it will fit onto the stage or, for that matter, into the specimen chamber. For special applications, very large stage–vacuum chamber combinations have been fabricated into which large forensic samples (such as boots or weapons) or 8-in diameter semiconductor wafers can be placed. For the latter case, special final lenses having conical shapes have been developed to allow for observation of large tilted samples at reasonably small working distances.

If the sample is an insulator there are still methods by which it can be studied in the instrument. The simplest approach is to coat it with a thin (10-nm) conducting film of carbon, gold, or some other metal. In following this approach, care must be taken to avoid artifacts and distortions that could be produced by nonuniform coatings or by agglomeration of the coating material. If an X-ray analysis is to be

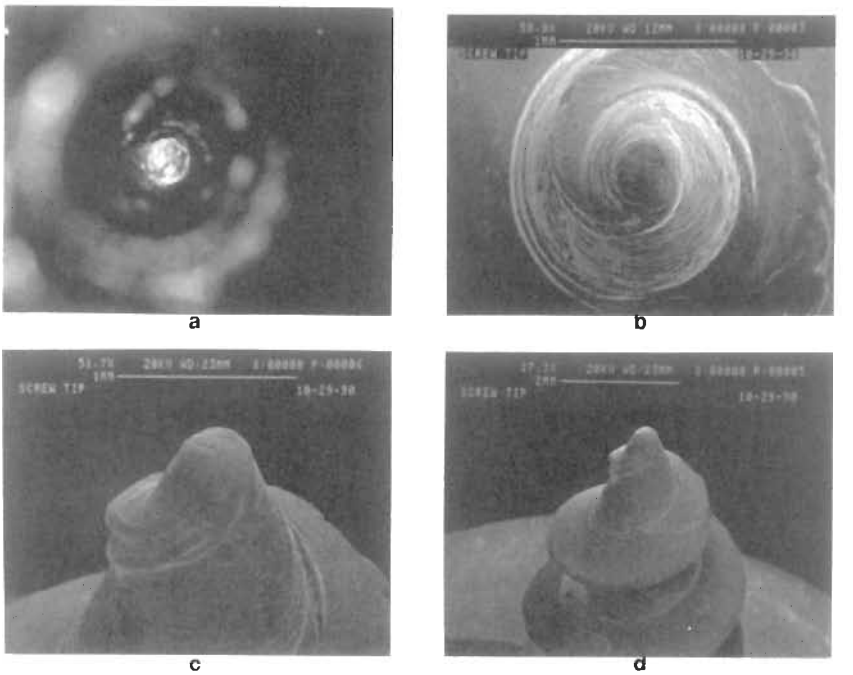

Figure 5 **Micrographs of a machine screw illustrating the great depth of field of the SEM: (a) optical micrograph of the very tip of the screw; (b) and (c) the same area in the SEM and a second image taken at an angle (the latter shows the depth of field quite clearly); (d) lower magnification image.**

made on such a coated surface, care must be taken to exclude or correct for any X-ray peaks generated in the deposited material.

Uncoated insulating samples also can be studied by using low primary beam voltages (< 2.0 keV) if one is willing to compromise image resolution to some extent. If we define the total electron yield as $\sigma = \delta + \eta$, then when $\sigma < 1$ we either must supply or remove electrons from the specimen to avoid charge build-up. Conduction to ground automatically takes care of this problem for conducting samples, but for insulators this does not occur. Consequently, one might expect it to be impossible to study insulating samples in the SEM. The way around this difficulty is suggested in Figure 6 which plots σ as a function of energy of the incident electron. The yield is seen to rise from 0 to some amount greater than 1 and then to decrease back below 1 as the energy increases. The two energy crossovers E_1 and E_2, between which minimal charging occurs, are often quite low, typically less than 2.0 keV.

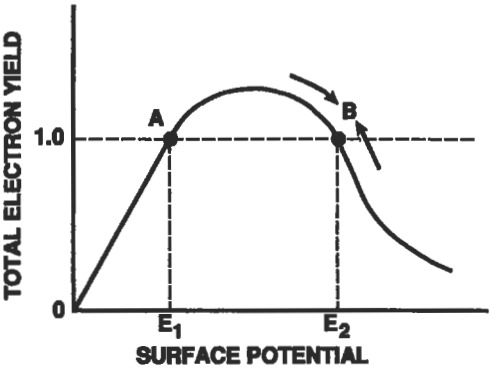

Figure 6 **Total electron yield as a function of the primary electron's energy when it arrives at the surface of the specimen.**

The energy scale in the figure is actually meant to depict the energy of the electron as it arrives at the surface. Because of charging, the electron's energy may be greater or less than the accelerating voltage would suggest. Consider electrons striking the surface with an energy near E_2 as identified by point B in the figure. If the energy is somewhat below that of the crossover point, the total electron yield will be greater than 1 and the surface will be positively charged, thereby attracting incoming electrons and increasing the effective energy of the primary beam. The electron's energy will continue to increase until E_2 is reached. If it overshoots, the yield will drop and some negative charging will begin until, again, a balance is reached at point B. Point B is therefore a stable operating point for the insulator in question, and operating around this point will allow excellent micrographs to be produced. E_1 (point A) does not represent a stable operating condition.

If the sample is a metal that has been coated with a thin oxide layer, a higher accelerating voltage might actually improve the image. The reason for this is that as the high-energy beam passes through the oxide, it can create electron–hole pairs in sufficient numbers to establish local conduction. This effect is often noted while observing semiconductor devices that have been passivated with thin deposited oxide films.

Applications

We have already discussed a number of applications of the SEM to materials characterization: topographical (SE) imaging, Energy-Dispersive X-Ray analysis (EDS) and the use of backscattering measurements to determine the composition of binary alloy systems. We now shall briefly discuss applications that are, in part, spe-

cific to certain industries or technologies. Although there is significant literature on applications of the SEM to the biological sciences, such applications will not be covered in this article.

At magnifications above a few thousand, the raster scanning of the beam is very linear, resulting in a constant magnification over the entire image. This is not the case at low magnifications, where significant nonlinearity may be present. Uniform magnification allows the image to be used for very precise size measurements. The SEM therefore can be a very accurate and precise metrology tool. This requires careful calibration using special SEM metrology standards available from the National Institute of Standards and Technology.

The fact that the SE coefficient varies in a known way with the angle that the primary beam makes with the surface allows the approximate determination of the depth (z) variation of the surface morphology from the information collected in a single image. By tilting the specimen slightly (5–8°), stereo pairs can be produced that provide excellent quality three-dimensional images via stereoscopic viewers. Software developments now allow these images to be calculated and displayed in three-dimension-like patterns on a computer screen. Contour maps can be generated in this way. The computer–SEM combination has been very valuable for the analysis of fracture surfaces and in studies of the topography of in-process integrated circuits and devices.

Computers can be used both for image analysis and image processing. In the former case, size distributions of particles or features, and their associated measurement parameters (area, circumference, maximum or minimum diameters, etc.) can be obtained easily because the image information is collected via digital scanning in a way that is directly compatible with the architecture of image analysis computers. In these systems an image is a stored array of 500×500 signal values. Larger arrays are also possible with larger memory capacity computers.

Image processing refers to the manipulation of the images themselves. This allows for mathematical smoothing, differentiation, and even image subtraction. The contrast and brightness in an image can be adjusted in a linear or nonlinear manner and algorithms exist to highlight edges of features or to completely suppress background variations. These methods allow the microscopist to extract the maximum amount of information from a single micrograph. As high-speed PCs and workstations continue to decrease in price while increasing in capacity, these applications will become more commonplace.

Electronics has, in fact, been a very fertile area for SEM application. The energy distribution of the SEs produced by a material in the SEM has been shown to shift linearly with the local potential of the surface. This phenomenon allows the SEM to be used in a noncontact way to measure voltages on the surfaces of semiconductor devices. This is accomplished using energy analysis of the SEs and by directly measuring these energy shifts. The measurements can be made very rapidly so that circuit waveforms at particular internal circuit nodes can be determined accurately.

Very high frequency operation of circuits can be observed by using stroboscopic techniques, blanking the primary beam at very high frequencies and by collecting information only during small portions of the operating cycle. By sliding the viewing window over the entire cycle, a waveform can be extracted with surprising sensitivity and temporal resolution. Recently, special SEM instruments have been designed that can observe high-speed devices under nominal operating conditions. The cost of these complex electron beam test systems can exceed $1,000,000.

Actually, any physical process that can be induced by the presence of an electron beam and that can generate a measurable signal can be used to produce an image in the SEM. For example, when a metal film is deposited on a clean semiconductor surface, a region of the semiconductor next to the metal can be depleted of mobile charge. This depletion region can develop a strong electric field. Imagine the metal to be connected through a current meter to the back side of the semiconductor surface. No current will flow, of course, but we can turn on an electron beam that penetrates the metal and allows the impinging electrons to create electron-hole pairs. The electric field will separate these carriers and sweep them out of the depletion region, thereby generating a current. Among other things, the current will be determined by the perfection or the chemistry of the spot where the beam strikes. By scanning the beam in the SEM mode, an image of the perfection (or chemistry) of the surface can be generated. This is referred to as electron beam-induced conductivity, and it has been used extensively to identify the kinds of defects that can affect semiconductor device operation.

The SEM can also be used to provide crystallographic information. Surfaces that to exhibit grain structure (fracture surfaces, etched, or decorated surfaces) can obviously be characterized as to grain size and shape. Electrons also can be channeled through a crystal lattice and when channeling occurs, fewer backscattered electrons can exit the surface. The channeling patterns so generated can be used to determine lattice parameters and strain.

The X-rays generated when an electron beam strikes a crystal also can be diffracted by the specimen in which they are produced. If a photograph is made of this diffraction pattern (the Kossel pattern) using a special camera, localized crystallographic information can be gleaned.

Further applications abound. Local magnetic fields affect the trajectories of the SEs as well as the BSEs, making the SEM a useful tool for observing the magnetic domains of ferromagnetic materials, magnetic tapes, and disk surfaces. Pulsed electron beams generate both thermal and acoustic signals which can be imaged to provide mechanical property maps of materials. Some semiconductors and oxides produce photons in the ultraviolet, visible, or infrared regions, and these cathodoluminescence signals provide valuable information about the electronic properties of these materials. The application of this method to semiconductor lasers or LED devices is probably self-evident. Even deep-level transient spectroscopy, a method that is particularly difficult to interpret and that provides information about impu-

rities having energy levels within the band gap of semiconductors, has been used to produce images in the SEM.

Conclusions

Every month a new application for the SEM appears in the literature, and there is no reason to assume that this growth will cease. The SEM is one of the more versatile of analytical instruments and it is often the first expensive instrument that a characterization laboratory will purchase.

As time goes on, the ultimate resolution of the SEM operated in these modes will probably level out near 1 nm. The major growth of SEMs now seems to be in the development of specialized instruments. An environmental SEM has been developed that uses differential pumping to permit the observation of specimens at higher pressures. Photographs of the formation of ice crystals have been taken and the instrument has particular application to samples that are not vacuum compatible, such as biological samples.

Other instruments have been described that have application in the electronics field. Special metallurgical hot and cold stages are being produced, and stages capable of large motions with sub-μm accuracy and reproducibility will become common.

Computers will be integrated more and more into commercial SEMs and there is an enormous potential for the growth of computer supported applications. At the same time, related instruments will be developed and extended, such as the scanning ion microscope, which uses liquid-metal ion sources to produce finely focused ion beams that can produce SEs and secondary ions for image generation. The contrast mechanisms that are exhibited in these instruments can provide new insights into materials analysis.

Related Articles in the Encyclopedia

TEM, STEM, EDS, EPMA, Surface Roughness, AES, and CL

References

1 J. I. Goldstein, Dale E. Newbury, P. Echlin, D. C. Joy, C. Fiori, and E. Lifshin. *Scanning Microscopy and X-Ray Microanalysis.* Plenum Press, New York, 1981. An excellent and widely ranging introductory textbook on scanning microscopy and related techniques. Some biological applications are also discussed.

2 D. Newbury, D. C. Joy, P. Echlin, C. E. Fiori, and J. I. Goldstein. *Advanced Scanning Electron Microscopy and X-Ray Microanalysis.* Plenum Press, New York, 1986. A continuation and expansion of Reference 1, *advanced* does not imply a higher level of difficulty.

3 L. Reimer. *Scanning Electron Microscopy.* Springer-Verlag, Berlin, 1985. An advanced text for experts, this is probably the most definitive work in the field.

4 D. B. Holt and D. C. Joy. *SEM Microcharacterization of Semiconductors.* Academic Press, London, 1989. A detailed examination of the applications of the SEM to semiconductor electronics.

5 John C. Russ. *Computer Assisted Microscopy.* Plenum Press, New York, 1990. A highly readable account of the applications of computers to SEMs and other imaging instruments.

2.3 STM and SFM

Scanning Tunneling Microscopy and Scanning Force Microscopy

REBECCA S. HOWLAND AND MICHAEL D. KIRK

Contents

Introduction

Scanning Tunneling Microscopy (STM) and its offspring, Scanning Force Microscopy (SFM), are real-space imaging techniques that can produce topographic images of a surface with atomic resolution in all three dimensions. Almost any solid surface can be studied with STM or SFM: insulators, semiconductors, and conductors, transparent as well as opaque materials. Surfaces can be studied in air, in liquid, or in ultrahigh vacuum, with fields of view from atoms to greater than 250 × 250 μm. With this flexibility in both the operating environment and types of samples that can be studied, STM / SFM is a powerful imaging system.

The scanning tunneling microscope was invented at IBM, Zurich, by Gerd Binnig and Heinrich Rohrer in 1981.[1] In ultrahigh vacuum, they were able to resolve the atomic positions of atoms on the surface of Si (111) that had undergone a 7 × 7 reconstruction (Figure 1). With this historic image they solved the puzzle of the atomic structure of this well studied surface, thereby establishing firmly the credibility and importance of this form of microscopy. For the invention of STM, Binnig and Rohrer earned the Nobel Prize for Physics in 1986.

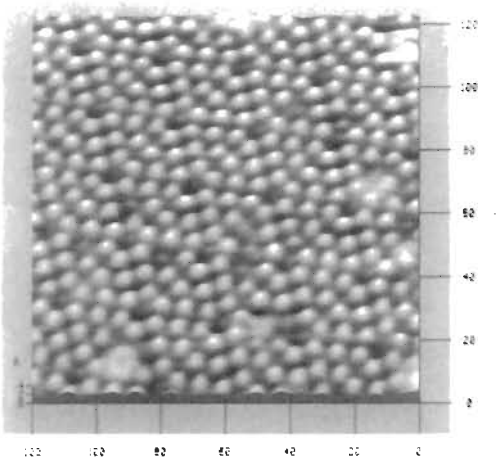

Figure 1 **Ultrahigh-vacuum STM image of Si (111) showing 7 × 7 reconstruction.**

Since then, STM has been established as an instrument for forefront research in surface physics. Atomic resolution work in ultrahigh vacuum includes studies of metals, semimetals and semiconductors. In particular, ultrahigh-vacuum STM has been used to elucidate the reconstructions that Si, as well as other semiconducting and metallic surfaces undergo when a submonolayer to a few monolayers of metals are adsorbed on the otherwise pristine surface.[2]

Because STM measures a quantum-mechanical tunneling current, the tip must be within a few Å of a conducting surface. Therefore any surface oxide or other contaminant will complicate operation under ambient conditions. Nevertheless, a great deal of work has been done in air, liquid, or at low temperatures on inert surfaces. Studies of adsorbed molecules on these surfaces (for example, liquid crystals on highly oriented, pyrolytic graphite[3]) have shown that STM is capable of even atomic resolution on organic materials.

The inability of STM to study insulators was addressed in 1985 when Binnig, Christoph Gerber and Calvin Quate invented a related instrument, the scanning force microscope.[4] Operation of SFM does not require a conducting surface; thus insulators can be studied without applying a destructive coating. Furthermore, studying surfaces in air is feasible, greatly simplifying sample preparation while reducing the cost and complexity of the microscope.

STM and SFM belong to an expanding family of instruments commonly termed Scanning Probe Microscopes (SPMs). Other common members include the magnetic force microscope, the scanning capacitance microscope, and the scanning acoustic microscope.[5]

Although the first six or seven years of scanning probe microscope history involved mostly atomic imaging, SPMs have evolved into tools complementary to Scanning and Transmission Electron Microscopes (SEMs and TEMs), and optical and stylus profilometers. The change was brought about chiefly by the introduction of the ambient SFM and by improvements in the range of the piezoelectric scanners that move the tip across the sample. With lateral scan ranges on the order of 250 μm, and vertical ranges of about 15 μm, STM and SFM can be used to address larger scale problems in surface science and engineering in addition to atomic-scale research. STM and SFM are commercially available, with several hundred units in place worldwide.

SPMs are simpler to operate than electron microscopes. Because the instruments can operate under ambient conditions, the set-up time can be a matter of minutes. Sample preparation is minimal. SFM does not require a conducting path, so samples can be mounted with double-stick tape. STM can use a sample holder with conducting clips, similar to that used for SEM. An image can be acquired in less than a minute; in fact, "movies" of ten frames per second have been demonstrated.[6]

The three-dimensional, quantitative nature of STM and SFM data permit in-depth statistical analysis of the surface that can include contributions from features 10 nm across or smaller. By contrast, optical and stylus profilometers average over areas a few hundred Å across at best, and more typically a μm. Vertical resolution for SFM/STM is sub-Å, better than that of other profilometers. STM and SFM are excellent high-resolution profilometers.

STM and SFM are free from many of the artifacts that afflict other kinds of profilometers. Optical profilometers can experience complicated phase shifts when materials with different optical properties are encountered. The SFM is sensitive to topography only, independent of the optical properties of the surface. (STM may be sensitive to the optical properties of the material inasmuch as optical properties are related to electronic structure.) The tips of traditional stylus profilometers exert forces that can damage the surfaces of soft materials, whereas the force on SFM tips is many orders of magnitude lower. SFM can image even the tracks left by other stylus profilometers.

In summary, scanning probe microscopes are research tools of increasing importance for atomic-imaging applications in surface science. In addition, SFM and STM are now used in many applications as complementary techniques to SEM, TEM, and optical and stylus profilometry. They meet or exceed the performance of these instruments under most conditions, and have the advantage of operating in an ambient environment with little or no sample preparation. The utility of scanning probe microscopy to the magnetic disk, semiconductor, and the polymer industries is gaining recognition rapidly. Further industrial applications include the analysis of optical components, mechanical parts, biological samples, and other areas where quality control of surfaces is important.

Basic Principles

STM

Scanning tunneling microscopes use an atomically sharp tip, usually made of tungsten or Pt-Ir. When the tip is within a few Å of the sample's surface, and a bias voltage V_t is applied between the sample and the tip, quantum-mechanical tunneling takes place across the gap. This tunneling current I_t depends exponentially on the separation d between the tip and the sample, and linearly on the local density of states. The exponential dependence of the magnitude of I_t upon d means that, in most cases, a single atom on the tip will image the single nearest atom on the sample surface.

The quality of STM images depends critically on the mechanical and electronic structure of the tip. Tungsten tips are sharpened by electrochemical etching, and can be used for a few hours in air, until they oxidize. On the other hand, Pt-Ir tips can be made by stretching a wire and cutting it on an angle with wire cutters. These tips are easy to make and slow to oxidize, but the resulting tip does not have as high an aspect ratio as a tungsten tip. As a result, Pt-Ir tips are not as useful for imaging large structures.

In its most common mode of operation, STM employs a piezoelectric transducer to scan the tip across the sample (Figure 2a). A feedback loop operates on the scanner to maintain a constant separation between the tip and the sample. Monitoring the position of the scanner provides a precise measurement of the tip's position in three dimensions. The precision of the piezoelectric scanning elements, together with the exponential dependence of I_t upon d means that STM is able to provide images of individual atoms.

Because the tunneling current also depends on the local density of states, STM can be used for spatially resolved spectroscopic measurements. When the component atomic species are known, STM can differentiate among them by recording and comparing multiple images taken at different bias voltages. One can ramp the bias voltage between the tip and the sample and record the corresponding change in the tunneling current to measure I versus V or dI/dV versus V at specific sites on the image to learn directly about the electronic properties of the surface. Such measurements give direct information on the local density of electronic states. This technique was pioneered by Hamers, et al., who used tunneling spectroscopy to map the local variations in the bonding structure between Si atoms on a reconstructed surface.[7]

On the other hand, the sensitivity of STM to electronic structure can lead to undesired artifacts when the surface is composed of regions of varying conductivity. For example, an area of lower conductivity will be represented as a dip in the image. If the surface is not well known, separating topographic effects from electronic effects can be difficult.

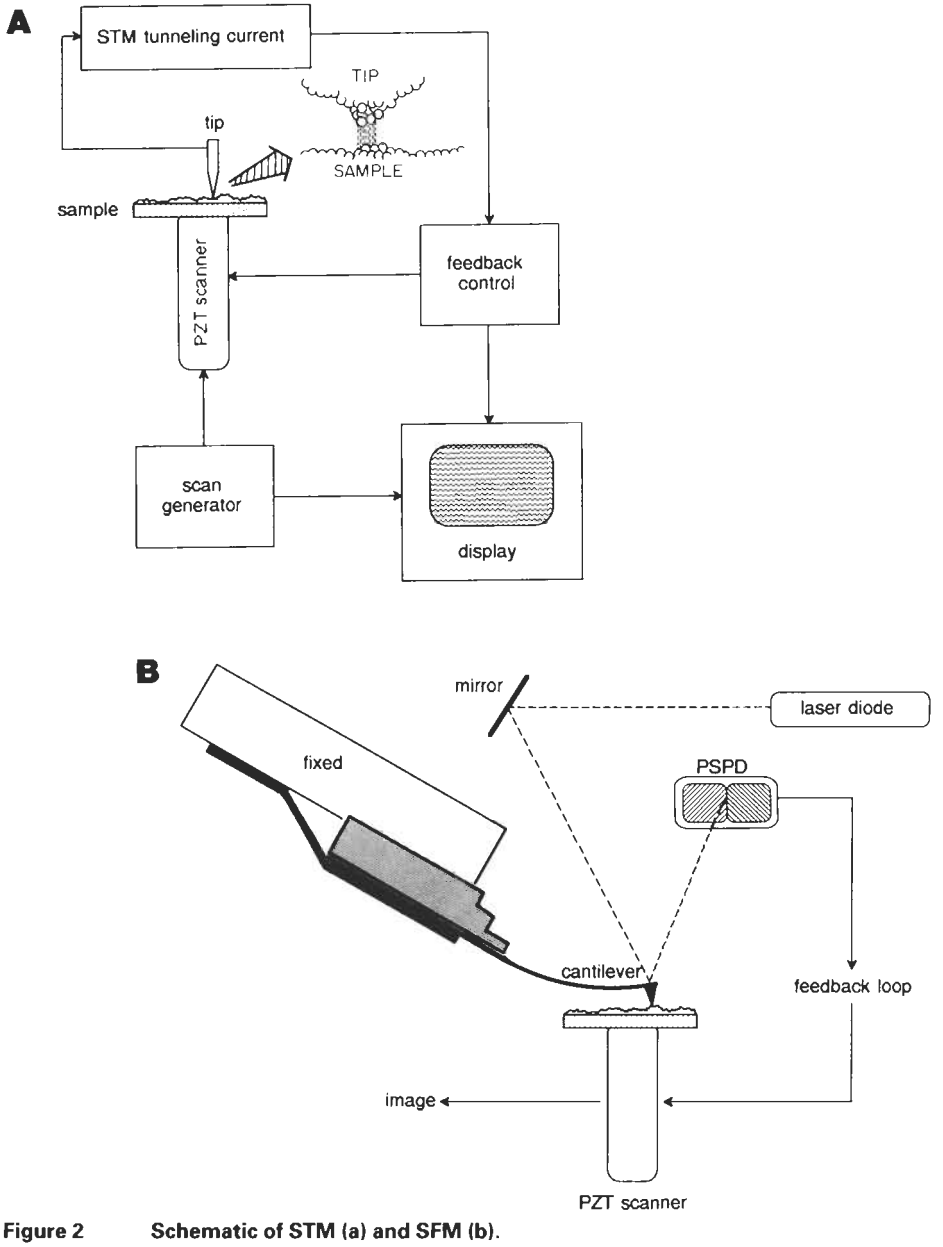

Figure 2 **Schematic of STM (a) and SFM (b).**

SFM

Scanning force microscopes use a sharp tip mounted on a flexible cantilever. When the tip comes within a few Å of the sample's surface, repulsive van der Waals forces

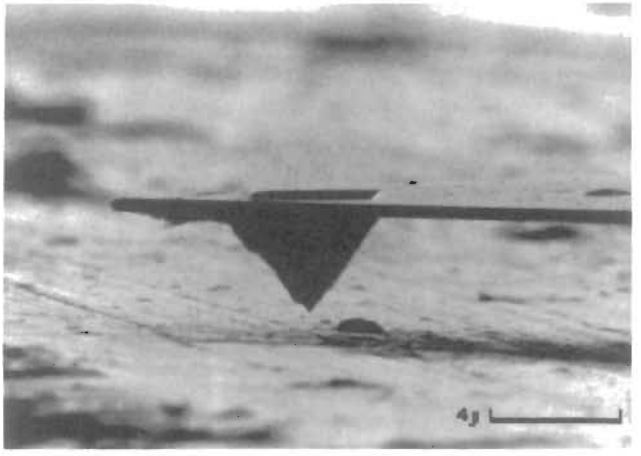

Figure 3 **SEM image of SFM cantilever showing pyramidal tip.**

between the atoms on the tip and those on the sample cause the cantilever to deflect. The magnitude of the deflection depends on the tip-to-sample distance *d*. However, this dependence is a power law, that is not as strong as the exponential dependence of the tunneling current upon *d* employed by STM. Thus several atoms on an SFM tip will interact with several atoms on the surface. Only with an unusually sharp tip and flat sample is the lateral resolution truly atomic; normally the lateral resolution of SFM is about 1nm.

Like STM, SFM employs a piezoelectric transducer to scan the tip across the sample (Figure 2b), and a feedback loop operates on the scanner to maintain a constant separation between the tip and the sample. As with STM, the image is generated by monitoring the position of the scanner in three dimensions.

For SFM, maintaining a constant separation between the tip and the sample means that the deflection of the cantilever must be measured accurately. The first SFM used an STM tip to tunnel to the back of the cantilever to measure its vertical deflection. However, this technique was sensitive to contaminants on the cantilever.[4] Optical methods proved more reliable. The most common method for monitoring the defection is with an optical-lever or beam-bounce detection system.[8] In this scheme, light from a laser diode is reflected from the back of the cantilever into a position-sensitive photodiode. A given cantilever deflection will then correspond to a specific position of the laser beam on the position-sensitive photodiode. Because the position-sensitive photodiode is very sensitive (about 0.1 Å), the vertical resolution of SFM is sub-Å.

Figure 3 shows an SEM micrograph of a typical SFM cantilever. The cantilevers are 100–200 μm long and 0.6 μm thick, microfabricated from low-stress Si_3N_4 with an integrated, pyramidal tip. Despite a minimal tip radius of about 400 Å,

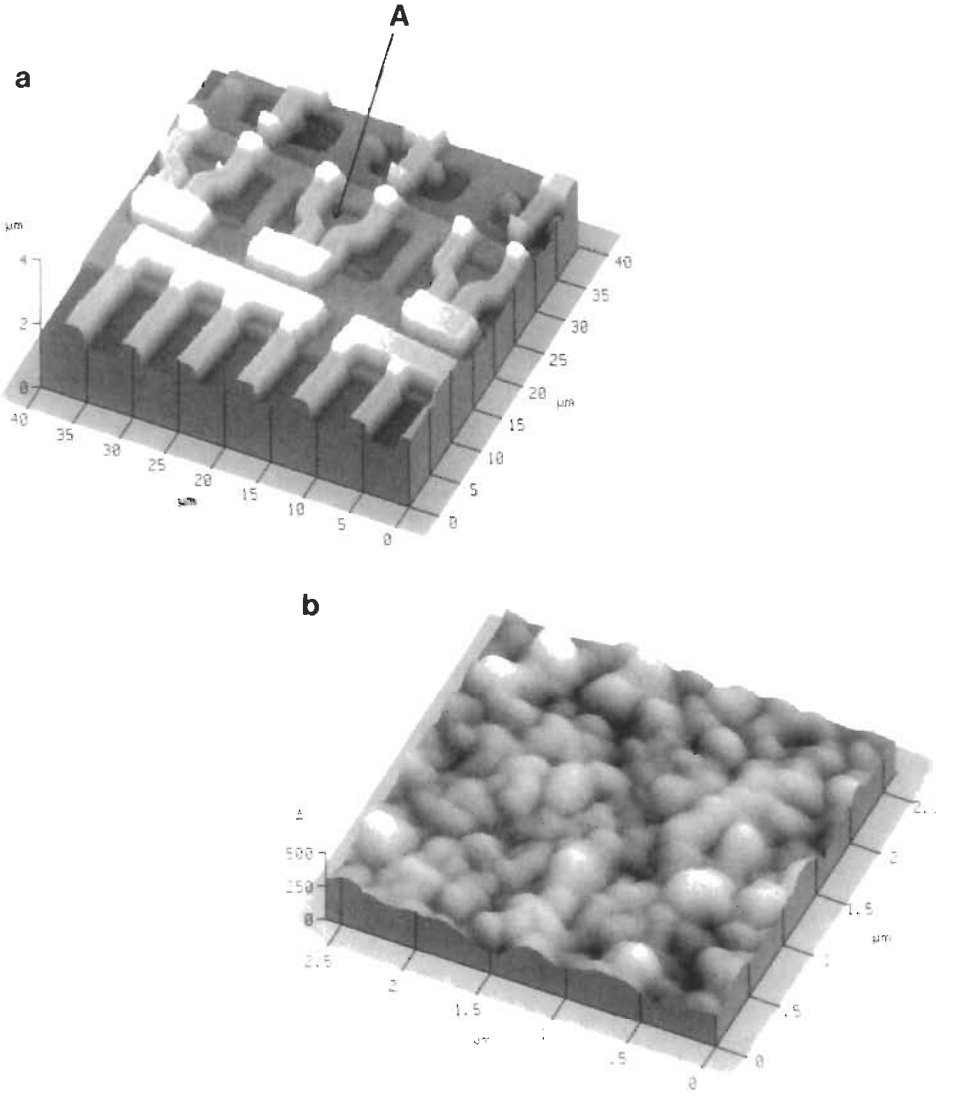

Figure 4 **SFM image of an integrated circuit (a) and close-up of silicon oxide on its surface (b).**

which is needed to achieve high lateral resolution, the pressure exerted on the sample surface is small because of the low force constant of the cantilever (typically 0.2 N / m), and the high sensitivity of the position-sensitive photodiode to cantilever deflection. The back of the cantilever may be coated with gold or another metal to enhance the reflectance of the laser beam into the detector.

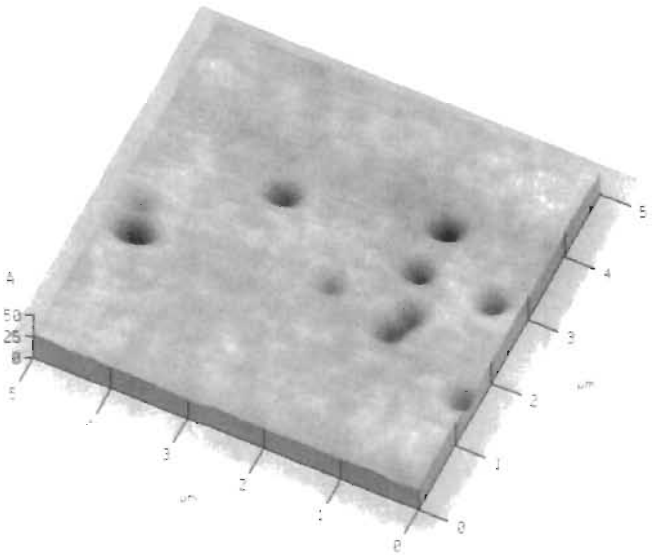

Figure 5 **SFM image of oxidized Si wafer showing pinhole defects 20 Å deep.**

Common Modes of Analysis and Examples

STM and SFM are most commonly used for topographic imaging, three-dimensional profilometry and spectroscopy (STM only).

Topography

Unlike optical or electron microscopes, which rely on shadowing to produce contrast that is related to height, STM and SFM provide topographic information that is truly three-dimensional. The data are digitally stored, allowing the computer to manipulate and display the data as a three-dimensional rendition, viewed from any altitude and azimuth. For example, Figure 4a shows an SFM image of an integrated circuit; Figure 4b is a close-up of the oxide on the surface of the chip in the region marked *A* in Figure 4a. In a similar application, Figure 5 is an SFM image of a Si wafer with pinholes, 20 Å deep. Easily imaged with SFM, these pinholes cannot be detected with SEM.

Profilometry

The three-dimensional, digital nature of SFM and STM data makes the instruments excellent high-resolution profilometers. Like traditional stylus or optical profilometers, scanning probe microscopes provide reliable height information. However, traditional profilometers scan in one dimension only and cannot match SPM's height and lateral resolution.

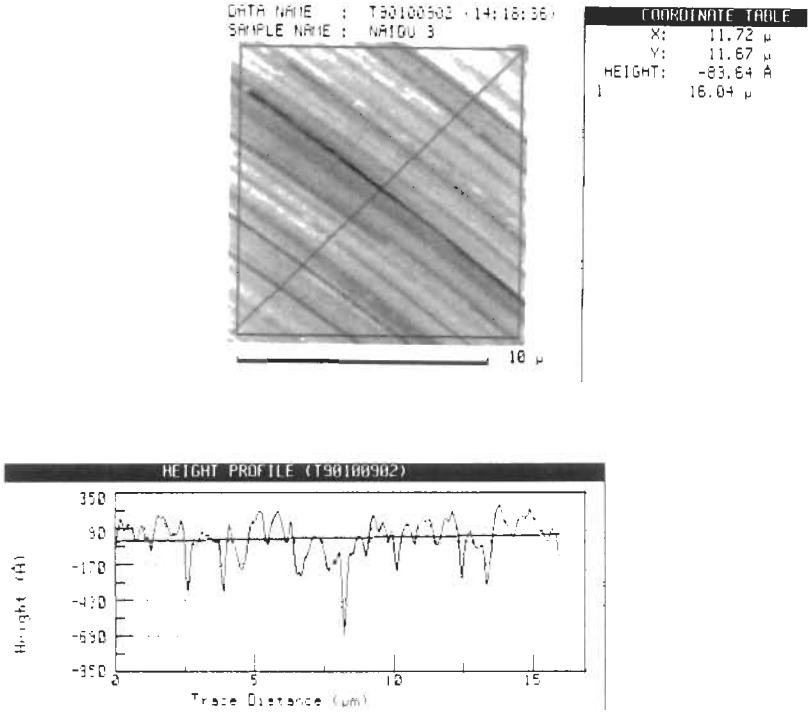

Figure 6 **SFM image of a magnetic storage disk demonstrating roughness analysis.**

In the magnetic storage disk industry, the technology has advanced to the point where surface roughness differences on the order of a few Å have become important. Optical and stylus profilometers, while still preferable for scanning very large distances, cannot measure contributions from small features. Figure 6 is an SFM image of a thin-film storage disk (top), shown top-down, with heights displayed in a linear intensity scale ("gray scale"). Using the mouse, the height profile of any cross section can be displayed and analyzed (bottom). Figure 7 shows a thin-film read–write head. The magnetic poles are recessed about 200 Å; their roughness is comparable to that of the surrounding medium. Note the textural difference between the glass embedding medium and the ceramic. SFM is not affected by differences in optical properties when it scans composite materials.

Profilometry of softer materials, such as polymers, is also possible with SFM, and with STM if the sample is conducting. Low forces on the SFM tip allow imaging of materials whose surfaces are degraded by traditional stylus profilometry. However, when the surface is soft enough that it deforms under pressure from the SFM tip, resolution will be degraded and topography may not be representative of the true

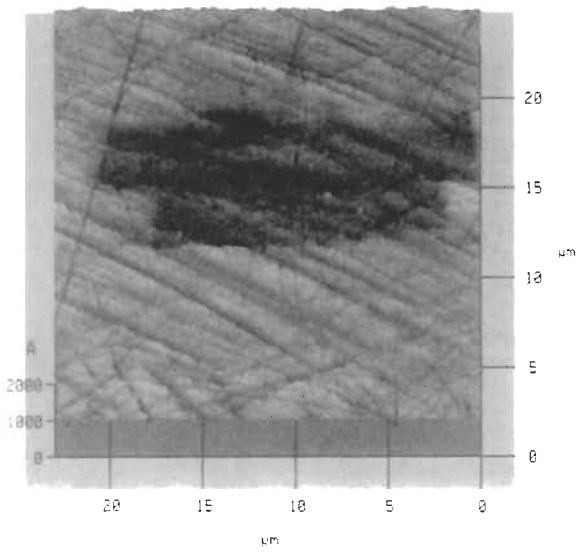

Figure 7 **SFM image of a thin-film read–write head showing magnetic poles (dark rectangles) recessed 200 Å.**

surface. One can investigate the reproducibility of the image by scanning the sample in different directions at various scan rates and image sizes.

Spectroscopy

The preceding topography and profilometry examples have focused on the scanning force microscope. STM also can be used for topographic imaging and profilometry, but the images will be convolutions of the topographic and electronic structure of the surface. A similar effect is seen with SEM, arising from differences in secondary electron coefficients among different materials.

Taking advantage of the sensitivity of the tunneling current to local electronic structure, the STM can be used to measure the spectra of surface-state densities directly. This can be accomplished by measuring the tunneling current as a function of the bias voltage between the tip and sample, or the conductivity, dI/dV, versus the bias voltage, at specific spatial locati ›ns on the surface. Figure 8 is a spectroscopic study of GaAs(110). The image on the left was taken with negative bias voltage on the STM tip, which allows tunneling into unoccupied states, thereby revealing the Ga atoms. Taken simultaneously but with a positive tip bias voltage, the image on the right results from tunneling out occupied states, and shows the positions of the As atoms.

The data above were collected in UHV environment to achieve the most pristine surface. Spectroscopy in air is usually more difficult to interpret due to contamination with oxides and other species, as is the case with all surface-sensitive spectroscopies.

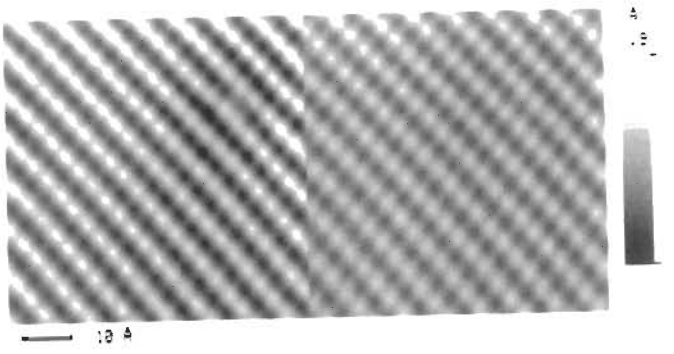

Figure 8 **Spectroscopic study of GaAs(110). With a positive voltage on the STM tip, the left-hand image represents As atoms, while the corresponding negative tip voltage on the right shows Ga atoms. (Courtesy of Y. Yang and J.H. Weaver, University of Minnesota)**

Sample Requirements

For atomic resolution an atomically flat sample is required to avoid tip imaging (see below). STM requires a conducting surface to establish the tunneling current. Doped Si has sufficient conductivity to enable STM imaging, but surfaces of lower conductivity may require a conductive coating. SFM can image surfaces of any conductivity. Both STM and SFM require solid surfaces that are somewhat rigid; otherwise the probes will deform the surfaces while scanning. Such deformation is easily diagnosed by repeatedly scanning the same area and noting changes.

The deformation of soft surfaces can be minimized with SFM by selecting cantilevers having a low force constant or by operating in an aqueous environment. The latter eliminates the viscous force that arises from the thin film of water that coats most surfaces in ambient environments. This viscous force is a large contributor to the total force on the tip. Its elimination means that the operating force in liquid can be reduced to the order of 10^{-9} N.

An example, Figure 9 is an SFM image of a Langmuir-Blodgett film. This film was polymerized with ultraviolet light, giving a periodicity of 200 Å, which is seen in the associated Fourier transform. The low forces exerted by the SFM tip are essential for imaging such soft polymer surfaces.

Poorly cleaned surfaces may not image well. While ordinary dry dust will be brushed aside by the tip and will not affect the image, oily or partially anchored dirt will deflect the SFM tip or interfere with the conductivity in STM. The result is usually a line smeared in the scan direction, exactly as one would expect if the tip began scanning something which moved as it was scanned. If the sample cannot be cleaned, the best procedure is to search for a clean area.

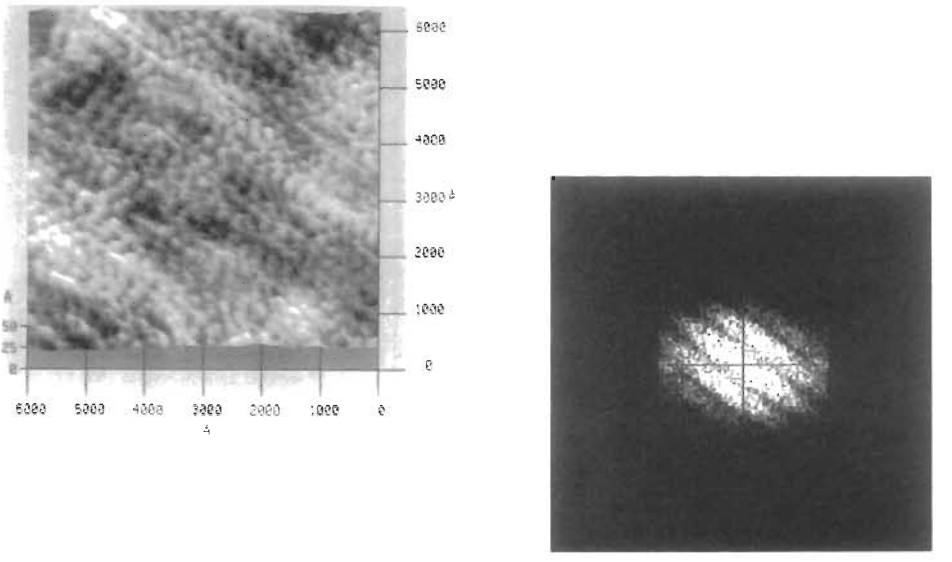

Figure 9 **SFM image of Langmuir-Blodgett film (top) and associated Fourier transform (bottom). (Courtesy of T. Kato, Utsunomiya University)**

Maximum sample sizes that can be accommodated by SFM or STM vary. Current systems can scan a 8-inch Si wafer without cutting it. When industry calls for the capability to scan larger samples, the SPM manufacturers are likely to respond.

Artifacts

The main body of artifacts in STM and SFM arises from a phenomenon known as *tip imaging*.[9] Every data point in a scan represents a convolution of the shape of the tip and the shape of the feature imaged, but as long as the tip is much sharper than the feature, the true edge profile of the feature is represented. However, when the feature is sharper than the tip, the image will be dominated by the edges of the tip. Fortunately, this kind of artifact is usually easy to identify.

Other artifacts that have been mentioned arise from the sensitivity of STM to local electronic structure, and the sensitivity of SFM to the rigidity of the sample's surface. Regions of variable conductivity will be convolved with topographic features in STM, and soft surfaces can deform under the pressure of the SFM tip. The latter can be addressed by operating SFM in the attractive mode, at some sacrifice in the lateral resolution. A limitation of both techniques is their inability to distinguish among atomic species, except in a limited number of circumstances with STM microscopy.

STM

In STM, the tip is formed by an atom or cluster of atoms at the end of a long wire. Because the dependence of the tunneling current upon the tip-to-sample distance is exponential, the closest atom on the tip will image the closest atom on the sample. If two atoms are equidistant from the surface, all of the features in the image will appear doubled. This is an example of multiple tip imaging. The best way to alleviate this problem is to collide the tip gently with the sample, to form a new tip and take another image. Alternatively, a voltage pulse can be applied to change the tip configuration by field emission.

STM tips will last for a day or so in ultrahigh vacuum. Most ultrahigh-vacuum STM systems provide storage for several tips so the chamber does not have to be vented just to change tips. In air, tips will oxidize more rapidly, but changing tips is a simple process.

SFM

At present, all commercial SFM tips are square pyramids, formed by CVD deposition of Si_3N_4 on an etch pit in (100) Si. The etch pit is bounded by (111) faces, which means that the resulting tip has an included angle of about 55°. Therefore the edge profiles of all features with sides steeper than 55° will be dominated by the profile of the tip.

Because many kinds of features have steep sides, tip imaging is a common plague of SFM images. One consolation is that the height of the feature will be reproduced accurately as long as the tip touches bottom between features. Thus the roughness statistics remain fairly accurate. The lateral dimensions, on the other hand, can provide the user with only an upper bound.

Another class of artifacts occurs when scanning vertical or undercut features. As the tip approaches a vertical surface, the side wall may encounter the feature before the end of the tip does. The resulting image will appear to contain a discontinuous shift. Changing the angle of the tip with respect to the sample's surface can minimize the problem. Side wall imaging also occurs in STM, but less frequently since an STM tip has a higher aspect ratio than that of an SFM tip.

Improving the aspect ratio of SFM tips is an area of active research. A major difficulty is that the durability of the tip likely will be compromised as aspect ratios are increased.

Conclusions

Scanning probe microscopy is a forefront technology that is well established for research in surface physics. STM and SFM are now emerging from university laboratories and gaining acceptance in several industrial markets. For topographic analysis and profilometry, the resolution and three-dimensional nature of the data is

unequalled by other techniques. The ease of use and nondestructive nature of the imaging are notable.

The main difficulty with STM and SFM techniques is the problem of tip imaging. Neither technique is recommended for obtaining accurate measurements of edge profiles of vertical or undercut surfaces. In addition, SFM tips cannot accurately image the lateral dimensions of features with sides steeper than 55° at present. Obtaining SFM tips with more suitable aspect ratios is an area of active research.

Scanning tunneling and scanning force microscopes are only two members of the family of scanning probe microscopes. Other types of scanning probe microscopes may become widely used in the near future. The magnetic force microscope, for example, may one day be used routinely to study magnetic domains in storage media.

Related Articles in the Encyclopedia

Light Microscopy, SEM, TEM, STEM, and Surface Roughness

References

1 G. Binnig, H. Rohrer, C. Gerber, and E. Weibel. *Phys. Rev. Lett.* **49,** 57, 1982.

2 D. Rugar and P. Hansma. *Physics Today*. October, 23, 1990.

3 J. S. Foster and J. E. Frommer. *Nature.* **333,** 542, 1988.

4 G. Binnig, C. F. Quate, and C. Gerber. *Phys. Rev. Lett.* **54,** 930, 1986.

5 H. K. Wickramsinghe. *Scientific American*. October, 98, 1989.

6 R. Barret and C. F. Quate. To be published.

7 R. J. Hamers, R. M. Tromp, and J. E. Demuth. *Phys. Rev. Lett.* **56,** 1972, 1986.

8 G. Meyer and N. M. Amer. *Appl. Phys. Lett.* **53,** 1045, 1988.

9 S.-I. Park, J. Nogami, and C. F. Quate. *Phys. Rev. B* **36,** 2863, 1987.

2.4 TEM

Transmission Electron Microscopy

KURT E. SICKAFUS

Contents

Introduction

Transmission Electron Microscopy (TEM) has, in three decades time, become a mainstay in the repertoire of characterization techniques for materials scientists. TEM's strong cards are its high lateral spatial resolution (better than 0.2 nm "point-to-point" on some instruments) and its capability to provide both image and diffraction information from a single sample. In addition, the highly energetic beam of electrons used in TEM interacts with sample matter to produce characteristic radiation and particles; these signals often are measured to provide materials characterization using EDS, EELS, EXELFS, backscattered and secondary electron imaging, to name a few possible techniques.

Basic Principles

In TEM, a focused electron beam is incident on a thin (less than 200 nm) sample. The signal in TEM is obtained from both undeflected and deflected electrons that penetrate the sample thickness. A series of magnetic lenses at and below the sample position are responsible for delivering the signal to a detector, usually a fluorescent screen, a film plate, or a video camera. Accompanying this signal transmission is a

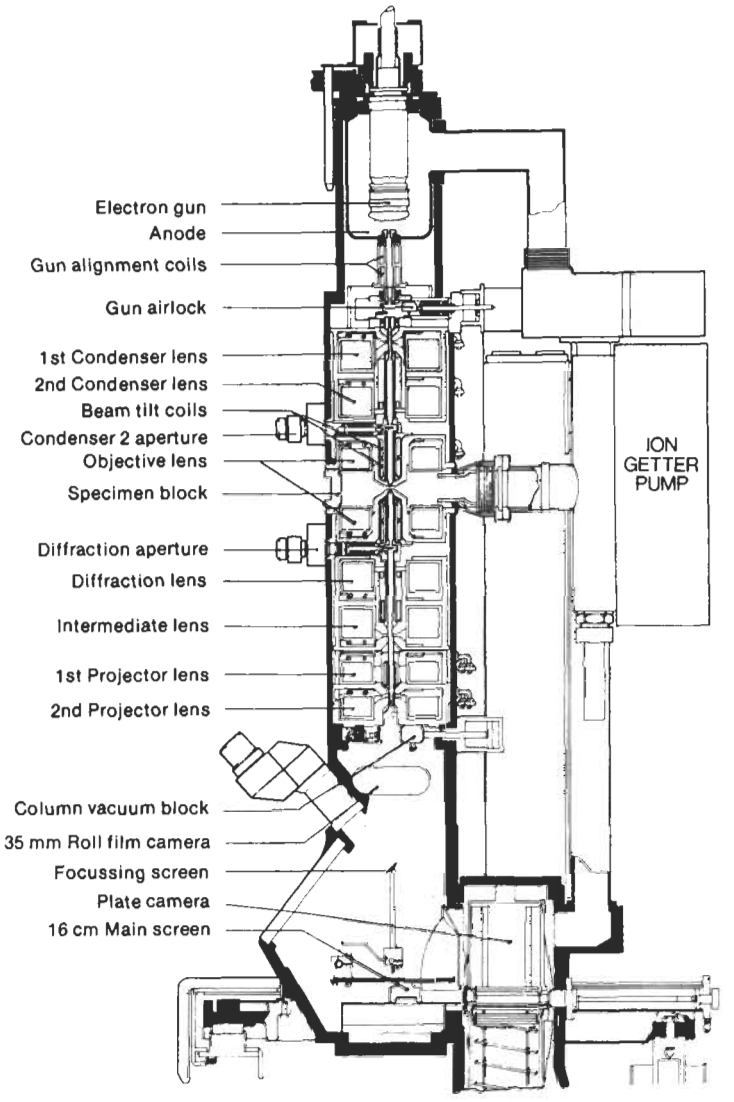

Figure 1a **Schematic diagram of a TEM instrument, showing the location of a thin sample and the principal lenses within a TEM column.**

magnification of the spatial information in the signal by as little as 50 times to as much as a factor of 10^6. This remarkable magnification range is facilitated by the small wavelength of the incident electrons, and is the key to the unique capabilities associated with TEM analysis. A schematic of a TEM instrument, showing the location of a thin sample and the principal lenses within a TEM column, is illustrated in Figure 1a.Figure 1b shows a schematic for the ray paths of both unscattered and scattered electrons beneath the sample.

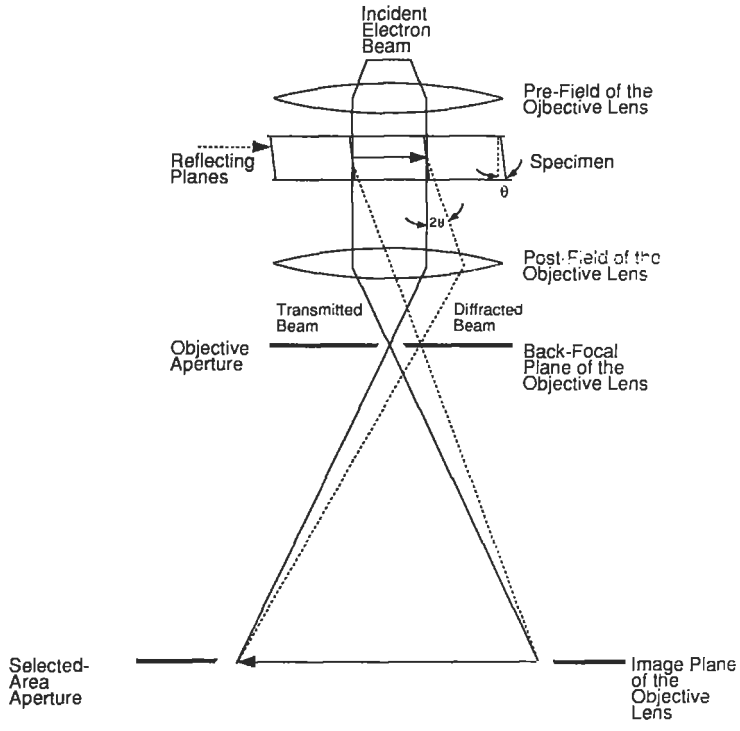

Figure 1b **Schematic representation for the ray paths of both unscattered and scattered electrons beneath the sample.**

Resolution

The high lateral spatial resolution in a TEM instrument is a consequence of several features of the technique. First, in the crudest sense, TEM has high spatial resolution because it uses a highly focused electron beam as a probe. This probe is focused at the specimen to a small spot, often a μm or less in diameter. More importantly, the probe's source is an electron gun designed to emit a highly coherent beam of monoenergetic electrons of exceedingly small wavelength. The wavelength, λ, of 100 keV electrons is only 0.0037 nm, much smaller than that of light, X rays, or neutrons used in other analytical techniques. Having such small wavelengths, since electrons in a TEM probe are in phase as they enter the specimen, their phase relationships upon exiting are correlated with spatial associations between scattering centers (atoms) within the material. Finally, high lateral spatial resolution is maintained via the use of extremely thin samples. In most TEM experiments, samples are thinned usually to less than 200 nm. For most materials this insures relatively few scattering events as each electron traverses the sample. Not only does this limit spreading of the probe, but much of the coherency of the incident source is also retained.

The higher the operating voltage of a TEM instrument, the greater its lateral spatial resolution. The theoretical instrumental point-to-point resolution is proportional[1] to $\lambda^{3/4}$. This suggests that simply going from a conventional TEM instrument operating at 100 kV to one operating at 400 kV should provide nearly a 50% reduction in the minimum resolvable spacing (λ is reduced from 0.0037 to 0.0016 nm in this case). Some commercially available 300 kV and 400 kV instruments, classified as *high-voltage* TEM instruments, have point-to-point resolutions better than 0.2 nm.

High-voltage TEM instruments have the additional advantage of greater electron penetration, because high-energy electrons interact less strongly with matter than low-energy electrons. So, it is possible to work with thicker samples on a high-voltage TEM. Electron penetration is determined by the mean distance between electron scattering events. The fewer the scattering events, either *elastic* (without energy loss) or *inelastic* (involving energy loss), the farther the electron can penetrate into the sample. For an Al sample, for instance, by going from a conventional 100-kV TEM instrument, to a high-voltage 400 kV TEM instrument, one can extend the mean distance between scattering events (both elastic and inelastic) by more than a factor of 2 (from 90 to 200 nm and from 30 to 70 nm, respectively, for elastic and inelastic scattering).[2] This not only allows the user to work with thicker samples but, at a given sample thickness, also reduces deleterious effects due to chromatic aberrations (since inelastic scattering is reduced).

One shortcoming of TEM is its limited depth resolution. Electron scattering information in a TEM image originates from a three-dimensional sample, but is *projected* onto a two-dimensional detector (a fluorescent screen, a film plate, or a CCD array coupled to a TV display). The collapse of the depth scale onto the plane of the detector necessarily implies that structural information along the beam direction is superimposed at the image plane. If two microstructural features are encountered by electrons traversing a sample, the resulting image contrast will be a convolution of scattering contrast from each of the objects. Conversely, to identify overlapping microstructural features in a given sample area, the image contrast from that sample region must be deconvolved.

In some cases, it is possible to obtain limited depth information using TEM. One way is to tilt the specimen to obtain a stereo image pair. Techniques also exist for determining the integrated depth (i.e., specimen thickness) of crystalline samples, e.g., using extinction contours in image mode or using convergent beam diffraction patterns. Alternatively, the width or trace of known defects, inclined to the surface of the foil, can be used to determine thickness from geometrical considerations. Secondary techniques, such as EELS and EDS can in some cases be used to measure thickness, either using plasmon loss peaks in the former case, or by modeling X-ray absorption characteristics in the latter. But no TEM study can escape consideration of the complications associated with depth.

Sensitivity

TEM has no inherent ability to distinguish atomic species. Nonetheless, electron scattering is exceedingly sensitive to the target element. Heavy atoms having large, positively charged nuclei, scatter electrons more effectively and to higher angles of deflection, than do light atoms. Electrons interact primarily with the potential field of an atomic nucleus, and to some extent the electron cloud surrounding the nucleus. The former is similar to the case for neutrons, though the principles of interaction are not related, while the latter is the case for X rays. The scattering of an electron by an atomic nucleus occurs by a Coulombic interaction known as Rutherford scattering. This is equivalent to the elastic scattering (without energy loss) mentioned earlier. The scattering of an electron by the electron cloud of an atom is most often an inelastic interaction (i.e., exhibiting energy loss). Energy loss accompanies scattering in this case because an electron in the incident beam matches the mass of a target electron orbiting an atomic nucleus. Hence, significant electron–electron momentum transfer is possible. A typical example of inelastic scattering in TEM is core-shell ionization of a target atom by an incoming electron. Such an ionization event contributes to the signal that is measured in Electron Energy Loss Spectroscopy (EELS) and is responsible for the characteristic X-Ray Fluorescence that is measured in Energy-Dispersive X-Ray Spectroscopy (EDS) and Wavelength-Dispersive X-Ray Spectroscopy (WDS). The latter two techniques differ only in the use of an energy-dispersive solid state detector versus a wavelength-dispersive crystal spectrometer.

The magnitude of the elastic electron–nucleus interaction scales with the charge on the nucleus, and so with atomic number Z. This property translates into image contrast in an electron micrograph (in the absence of diffraction contrast), to the extent that regions of high-Z appear darker than low-Z matrix material in conventional *bright-field* microscopy. This is illustrated in the bright-field TEM image in Figure 2, where high-Z, polyether sulfone ($-[C_6H_4-SO_2-C_6H_4-O-]_{-n}$) inclusions are seen as dark objects on a lighter background from a low-Z, polystyrene ($-[CH_2-CH(C_6H_5)-]_{-n}$) matrix. [The meaning of bright field is explained later in this article.]

The probability of interaction with a target atom is much greater for electrons than for X rays, with $f_e \sim 10^4 f_x$ (f_e is the electron atomic scattering factor and f_x is X-ray atomic scattering factor; each is a measure of elemental scattering efficiency or equivalently, the elemental sensitivity of the measurement).[3] Unfortunately, with this benefit of elemental sensitivity comes the undesirable feature of multiple scattering. The strong interaction of an incident electron with the potential field of a target atom means that numerous scattering events are possible as the electron traverses the sample. Each scattering event causes an angular deflection of the electron, and often this is accompanied by a loss of energy. The angular deflection upon scattering effectively diminishes the localization of the spatial information in the

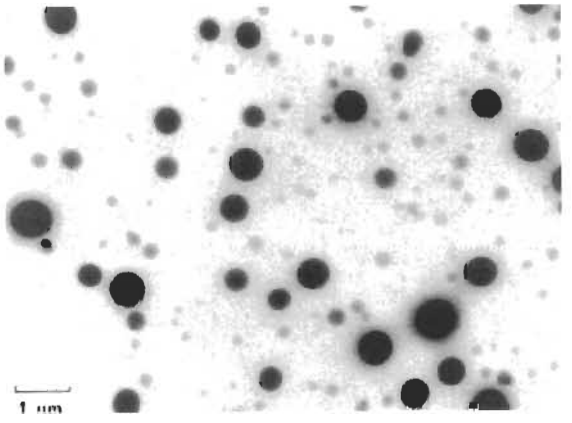

Figure 2 **Bright-field TEM image of polyether sulphone inclusions (dark objects; see arrows) in a polystyrene matrix.**

TEM signal; the energy losses upon scattering accentuate chromatic aberration effects.

The enormous sensitivity in an electron scattering experiment, in conjunction with the use of a high-brightness electron gun, leads to one of TEM's important features, that of real-time observation. In a conventional TEM, real-time observation is realized by using a W-filament source capable of delivering ~2×10^{19} electrons/cm^2-s to the specimen,[4] and a scintillating fluorescent screen to detect the transmitted electrons, viewed through a glass-window flange at the base of the microscope. Recent variations on this theme include the use of better vacuum systems that can accommodate LaB_6 or field-emission gun sources of higher brightness (up to ~6×10^{21} electrons/cm^2-s),[4] as well as the use of CCD array–TV displays to enhance detection sensitivity.

TEM Operation

TEM offers two methods of specimen observation, diffraction mode and image mode. In diffraction mode, an electron diffraction pattern is obtained on the fluorescent screen, originating from the sample area illuminated by the electron beam. The diffraction pattern is entirely equivalent to an X-ray diffraction pattern: a single crystal will produce a spot pattern on the screen, a polycrystal will produce a powder or ring pattern (assuming the illuminated area includes a sufficient quantity of crystallites), and a glassy or amorphous material will produce a series of diffuse halos.

The examples in Figure 3 illustrate these possibilities. Figure 3a shows a diffraction pattern from a single crystal Fe thin film, oriented with the [001] crystal axis

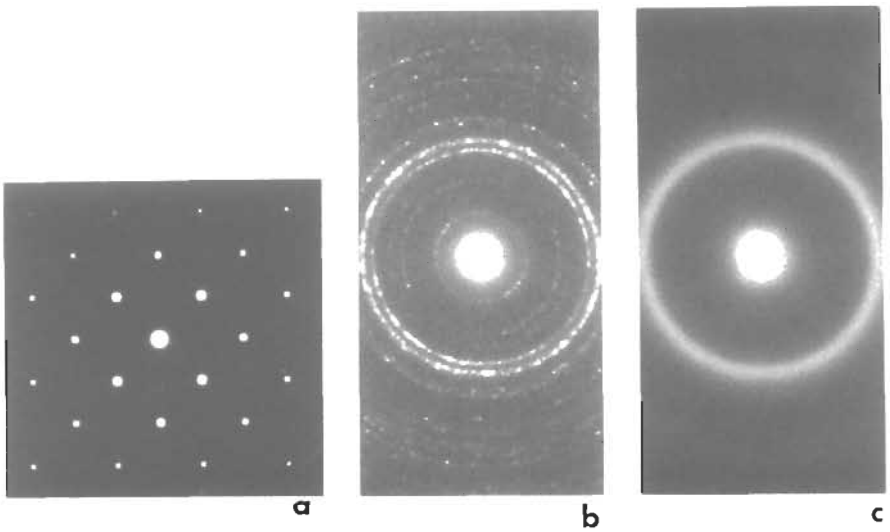

Figure 3 **(a) Diffraction pattern from a single crystal Fe thin film, oriented with the [001] crystal axis parallel to the incident electron beam direction. (b) Diffraction pattern from a polycrystalline thin film of Pd_2Si. (c) Diffraction pattern from the same film as in (c), following irradiation of the film with 400-keV Kr^+ ions. See text for discussion (b, c Courtesy of M. Nastasi, Los Alamos National Laboratory)**

parallel to the incident electron beam direction. This single crystal produces a characteristic spot pattern. In this case, the four-fold symmetry of the diffraction pattern is indicative of the symmetry of this body-centered cubic lattice. Figure 3b shows a ring pattern from a polycrystalline thin film, Pd_2Si. Figure 3c shows a diffuse halo diffraction pattern from the same film, following irradiation of the film with 400-keV Kr^+ ions. The diffuse halos (the second-order halo here is very faint) are indicative of scattering from an amorphous material, demonstrating a dramatic disordering of Pd_2Si crystal lattice by the Kr^+ ions.

The image mode produces an image of the illuminated sample area, as in Figure 2. The image can contain contrast brought about by several mechanisms: mass contrast, due to spatial separations between distinct atomic constituents; thickness contrast, due to nonuniformity in sample thickness; diffraction contrast, which in the case of crystalline materials results from scattering of the incident electron wave by structural defects; and phase contrast (see discussion later in this article). Alternating between image and diffraction mode on a TEM involves nothing more than the flick of a switch. The reasons for this simplicity are buried in the intricate electron optics technology that makes the practice of TEM possible.

Electron Optics

It is easiest to discuss the electron optics of a TEM instrument by addressing the instrument from top to bottom. Refer again to the schematic in Figure 1a. At the top of the TEM column is an electron source or gun. An electrostatic lens is used to accelerate electrons emitted by the filament to a high potential (typically 100–1,000 kV) and to focus the electrons to a cross-over just above the anode (the diameter of the cross-over image can be from 0.5 to 30 μm, depending on the type of gun[4]). The electrons at the cross-over image of the filament are delivered to the specimen by the next set of lenses on the column, the condensers.

Most modern TEMs use a two-stage condenser lens system that makes it possible to

1 Produce a highly demagnified image of cross-over at the specimen, such that only a very small sample region is illuminated (typically < 1 μm).

2 Focus the beam at "infinity" to produce nearly parallel illumination at the specimen.

The former procedure is the method of choice during operation in the image mode, while the latter condition is desirable for maximizing source coherency in the diffraction mode.

The specimen is immersed in the next lens encountered along the column, the objective lens. The objective lens is a magnetic lens, the design of which is the most crucial of all lenses on the instrument. Instrumental resolution is limited primarily by the spherical aberration of the objective lens.

The magnetic field at the center of the objective lens near the specimen position is large, typically 2–2.5 T (20–25 kG).[4] This places certain restrictions on TEMs applicability to studies of magnetic materials, particularly where high spatial resolution measurements are desired. Nevertheless, low-magnification TEM is often used to study magnetic domain characteristics in magnetic materials, using so-called Lorentz microscopy procedures.[5] In such instances, the objective lens is weakly excited, so that the incident electrons "see" mainly the magnetic field due to the specimen. Changes in this field across domain boundaries produce contrast in the transmitted image.

The final set of magnetic lenses beneath the specimen are jointly referred to as post-specimen lenses. Their primary task is to magnify the signal transferred by the objective lens. Modern instruments typically contain four post-specimen lenses: diffraction, intermediate, projector 1, and projector 2 (in order of appearance below the specimen). They provide a TEM with its tremendous magnification flexibility.

Collectively, the post-specimen lenses serve one of two purposes: they magnify either the diffraction pattern from the sample produced at the back focal plane of the objective lens; or they magnify the image produced at the image plane of the objective lens. These optical planes are illustrated in the electron ray diagram in

Figure 1b. By varying the lenses' strengths so as to alternate between these two object planes, the post-specimen lenses deliver either a magnified diffraction pattern or a magnified image of the specimen to the detector.

The primary remaining considerations regarding the TEM column are the diaphragms or apertures employed at certain positions along the column. The purpose of these apertures is to filter either the source or the transmitted signal. The most important diaphragm is called the objective aperture. This aperture lies in the back focal plane of the objective lens. In this plane the scattered electron waves recombine to form a diffraction pattern. A diffraction pattern corresponds to the angular dispersion of the electron intensity removed from the incident beam by interaction with the specimen. Inserting an aperture in this plane effectively blocks certain scattered waves. The larger the objective aperture, the greater the angular dispersion that is accepted in the transmitted signal. Figure 1b shows an example where the undeflected or transmitted beam is passed by the objective aperture, while the first-order, Bragg-diffracted beam is blocked. Consequently, only intensity in the transmitted beam can contribute to the image formed at the image plane of the objective lens. Use of a small objective aperture while operating in the image mode, which blocks all diffracted beams (as in this example), can serve to enhance significantly image contrast. Use of a large objective aperture, that allows the passage of many diffracted beams, is the *modus operandi* for the technique referred to as high-resolution transmission electron microscopy (HRTEM), discussed later in this article.

Diffraction Mode

A TEM provides the means to obtain a diffraction pattern from a small specimen area. This diffraction pattern is obtained in diffraction mode, where the post-specimen lenses are set to examine the information in the transmitted signal at the back focal plane of the objective lens.

Figure 4 illustrates some of the important aspects of diffraction in TEM. Figure 4a shows a micrograph obtained in image mode of a small region of a Ni_3Al sample illuminated by an electron beam, containing lamellar crystallites with well-defined orientation relationships. Figure 4b shows a selected-area diffraction (SAD) pattern from the same region. In SAD, the condenser lens is defocused to produce parallel illumination at the specimen and a selected-area aperture (see Figure 1b) is used to limit the diffracting volume. Many spots, or reflections, are evident in this pattern, due in part to the special orientation of the sample. The SAD pattern is a superposition of diffraction patterns from crystallites in the illuminated area that possess distinct orientations.

Figures 4c and 4d illustrate what happens when the incident electron probe is focused to illuminate alternately a crystallite in the center of the image (labelled *twin*) (Figure 4c) and another crystallite adjacent to the twin (Figure 4d). This focused-probe technique is sometimes referred to as *micro-diffraction*. Two effects are evident in these micro-diffraction patterns. First, the diffraction patterns consist

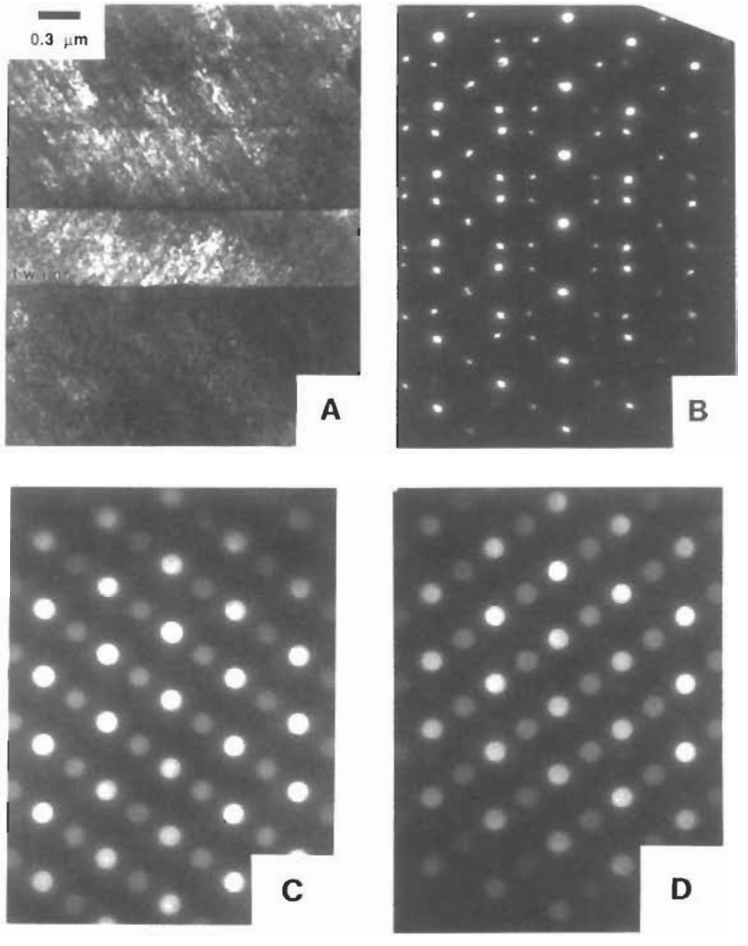

Figure 4 **(a) Bright-field image from a small region of a Ni_3Al sample containing oriented crystallites in the center of the illuminated area (one crystallite is labeled *twin* on the micrograph). (b) Selected-area diffraction (SAD) pattern from the same region as in (a). (c) Microdiffraction pattern from the middle region in (a) containing the twin crystallite. (d) Microdiffraction pattern from a crystallite adjacent to the *twin* in (a, c). (Courtesy of G. T. Gray III, Los Alamos National Laboratory)**

of "discs" instead of spots. This is a consequence of the use of focused or convergent illumination instead of parallel illumination. Second, the number of reflections in each of these patterns is reduced from that of the SAD pattern in Figure 4b (the reflections are no longer paired). But a superposition of the reflected discs in the microdiffraction patterns can account for all the reflections observed in the SAD pattern. This illustrates the flexibility of a TEM to obtain diffraction information

from exceedingly small areas of a sample (in this case, a region of diameter about 0.5 μm or less).

The example in Figure 4 illustrates that the diffraction pattern produced by a crystalline specimen depends on the orientation of the crystal with respect to the incident beam. This is analogous to the way a Laue pattern varies upon changing the orientation of a diffracting crystal relative to an X-ray source.[6] In TEM, this orientation may be varied using the sample manipulation capabilities of a tilting specimen holder. Holders come with a range of tilt capabilities, including single-axis tilt, double-axis tilt, and tilt–rotate stages, with up to ±60° tilting capabilities. But the higher the resolution of the instrument, the more limited the tilting capabilities of a tilt stage (to as low as ±10°). For studies of single crystals or epitaxial thin films, it is important to have access to as much tilt capability as possible.

SAD patterns often are used to determine the Bravais lattice and lattice parameters of crystalline materials. Lattice parameter measurements are made by the same procedures used in X-ray diffraction.[6] Using SAD, each diffracted scattering angle θ is measured in an SAD pattern and an associated atomic interplanar spacing d determined using Bragg's Law, $\lambda = 2d \sin \theta$. Note that at the small electron wavelengths of TEM, typical θ values are small quantities, only 9 mrad for a Au (200) reflection using 100-keV electrons ($\lambda = 0.0037$ nm). By comparison, in a LEED experiment using 150 eV electrons, since $\lambda = 0.1$ nm, a Au (200) reflection would appear at $\theta = 500$ mrad or 30°, using $\lambda = d \sin \theta$; such a large scattering angle is easily observed using the optics of a LEED system, which uses no magnifying lenses for the scattered electrons. Because of the extremely small angle scattering situation in TEM, observation of diffraction patterns is made possible only with the use of magnifying, post-specimen lenses. These lenses greatly magnify the diffraction pattern.

The crystal group or Bravais lattice of an unknown crystalline material can also be obtained using SAD. This is achieved easily with polycrystalline specimens, employing the same powder pattern "indexing" procedures as are used in X-ray diffraction.[6]

Image Mode

In image mode, the post-specimen lenses are set to examine the information in the transmitted signal at the image plane of the objective lens. Here, the scattered electron waves finally recombine, forming an image with recognizable details related to the sample microstructure (or atomic structure).

There are three primary image modes that are used in conventional TEM work, bright-field microscopy, dark-field microscopy, and high-resolution electron microscopy. In practice, the three image modes differ in the way in which an objective diaphragm is used as a filter in the back focal plane.

In bright-field microscopy, a small objective aperture is used to block all diffracted beams and to pass only the transmitted (undiffracted) electron beam. In the

absence of any microstructural defects, a bright-field image of a strain-free, single-phase material of uniform thickness, would lack contrast regardless of specimen orientation. Contrast arises in a bright-field image when thickness or compositional variations or structural anomalies are present in the illuminated sample area (or when the sample is strained), so that electrons in some areas are scattered out of the primary beam to a greater extent than in neighboring regions. Regions in which intensity is most effectively removed from the incident beam to become scattered or diffracted intensity appear dark in a bright-field image since this intensity is removed by the objective diaphragm. The images in Figure 2 were obtained using the bright-field imaging procedures.

In multiphase, amorphous or glassy materials, regions containing a phase of high average Z will scatter electrons more efficiently and to higher angles than regions containing a low average Z. The objective aperture in bright-field blocks this scattered intensity, making the high-Z material appear darker (less transmitted intensity) than the low-Z material. This is *mass* contrast, due primarily to incoherent elastic scattering. The scattering is largely incoherent because spatial relationships between scattering centers in these materials are not periodic. A priori there are no well-defined phase relationships between electrons scattered by such materials. Under these circumstances, the transmitted intensity distribution is determined from the principle of the additivity of individual scattered intensities, without consideration for the individual scattered amplitudes.

In crystalline materials, dark contrast regions in bright-field usually originate from areas that are aligned for Bragg diffraction. Here, intensity is removed from the transmitted beam to produce diffracted intensity, that subsequently is blocked by the objective aperture. This is *diffraction* contrast, due to coherent elastic scattering. The scattering is coherent because of the periodic arrangement of scattering centers in crystalline materials. In this case, the transmitted intensity distribution depends on the superposition of the individual scattered amplitudes.

Diffraction contrast is often observed in the vicinity of defects in the lattice. The origins of this contrast are illustrated in Figure 5. Figure 5a shows a thin sample with atomic planes that are close to a Bragg diffraction orientation, but are actually unaligned with respect to an electron beam propagating down the optic axis of the microscope. On the lefthand side of the diagram, the atomic planes are undistorted, as they would be in a perfect crystal. On the righthand side of the diagram, the sample contains an edge dislocation in the middle of the sample thickness. The dislocation lies normal to the page so that it appears in this diagram in cross section. Near the core of the dislocation, the atomic planes are distorted or bent to accommodate the strains associated with the atomic displacements at the dislocation core. See Figure 5a. The result of these local distortions is that some planes near the core adopt a Bragg orientation with respect to the incident beam. This is shown schematically in Figure 5b, where the incident and transmitted electron ray paths are shown for the same sample region. The undistorted crystal on the lefthand side, which is not in

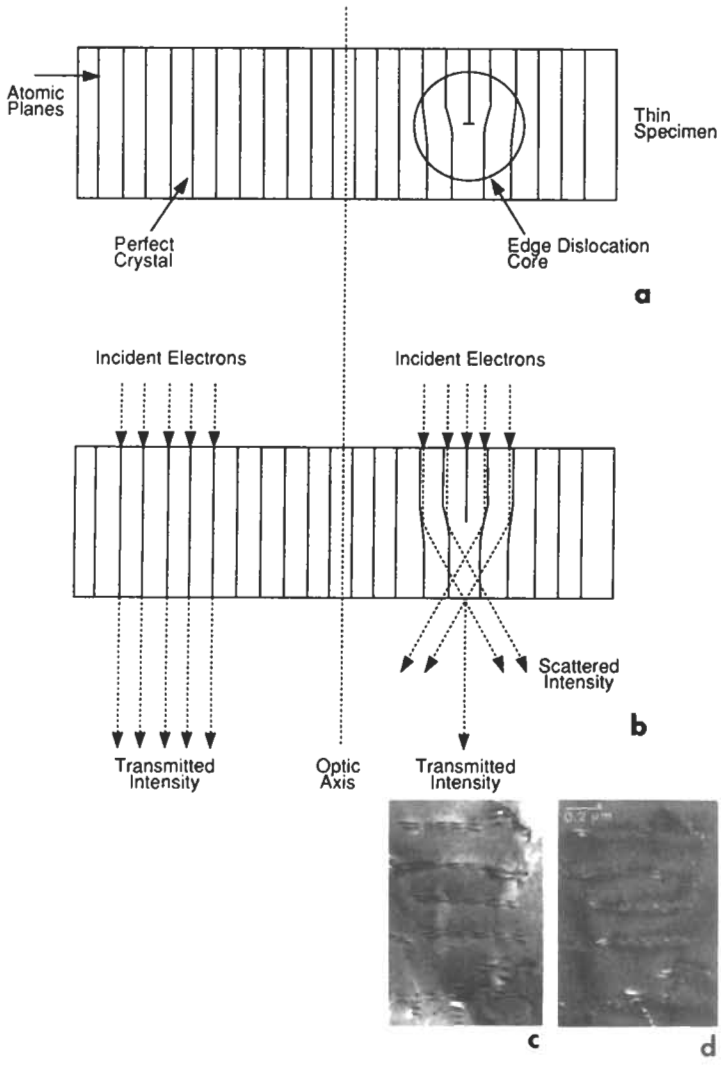

Figure 5 **(a) Schematic of a thin sample with atomic planes that are close to a Bragg diffraction orientation, but which are unaligned with respect to an electron beam propagating down the optic axis of the microscope. The sample contains an edge dislocation in the middle of the sample thickness on the right-hand side of the diagram. (b) Incident and transmitted electron ray paths for electron scattering from the same sample region in (a). (c) Bright-field image of dislocations in shock-deformed Ni_3Al. (d) Dark-field image from the same region as in (c). (c, d courtesy of H. W. Sizek, Los Alamos National Laboratory)**

Bragg alignment, is shown as simply transmitting a similar magnitude of undeflected intensity. The region containing the dislocation, on the other hand, is

shown with a deficiency of undeflected, transmitted intensity, because considerable Bragg diffraction occurs near the core of the dislocation. Diffraction is represented by the scattered rays shown in the diagram, which are subsequently blocked by the objective aperture in the bright-field mode. In a bright-field image from this sample, the region containing the edge dislocation would appear dark, surrounded by bright intensity from the neighboring, undistorted crystalline material. In this case, contrast in the image would appear as a dark line across the bright-field image, since this dislocation line lies parallel to the plane of the sample.

This situation is illustrated by the bright-field image in Figure 5c, where a set of dislocations in shock-deformed Ni_3Al is imaged. Each dislocation appears as a dark line on a bright background (each line appears paired in this image because these are dissociated superlattice dislocations). By comparison, Figure 5d is a dark-field image from the same region, which was obtained by placing the objective aperture around a diffracted beam in the SAD pattern instead of the transmitted beam. The same dislocations that were imaged in the bright-field mode in Figure 5c now appear as bright lines on a dark background. The dark background results because the undistorted crystal lattice is not well-aligned for diffraction, so little scattered intensity arises from these regions, to contribute brightness to this dark-field image. But the dislocations appear bright since diffracted intensity from the dislocation cores (that was lost in the bright-field mode) is now captured in the dark-field mode. This is typical of image contrast in the dark-field mode; consequently the name dark-field (i.e., bright objects on a dark background) is applied to this imaging technique. Dark-field microscopy is a powerful technique, but many associated subtleties complicate its practice. A most noteworthy example is the technique of weak-beam dark-field imaging.[5]

The last example of imaging techniques in TEM is high-resolution transmission electron microscopy. High-resolution TEM is made possible by using a large-diameter objective diaphragm that admits not only the transmitted beam, but at least one diffracted beam as well. All of the beams passed by the objective aperture are then made to recombine in the image-forming process, in such a way that their amplitudes and phases are preserved. When viewed at high-magnification, it is possible to see contrast in the image in the form of periodic fringes. These fringes represent direct resolution of the Bragg diffracting planes; the contrast is referred to as *phase* contrast. The fringes that are visible in the high-resolution image originate from those planes that are oriented as Bragg reflecting planes and that possess interplanar spacings greater than the lateral spatial resolution limits of the instrument. The principle here is the same as in the Abbé theory for scattering from gratings in light optics.[7] An example of an HRTEM image is shown in Figure 6. This image is of an epitaxial thin film of $Y_1Ba_2Cu_3O_{7-x}$ grown on $LaAlO_3$ (shown in cross section).

The HRTEM technique has become popular in recent years due to the more common availability of high-voltage TEMs with spatial resolutions in excess of

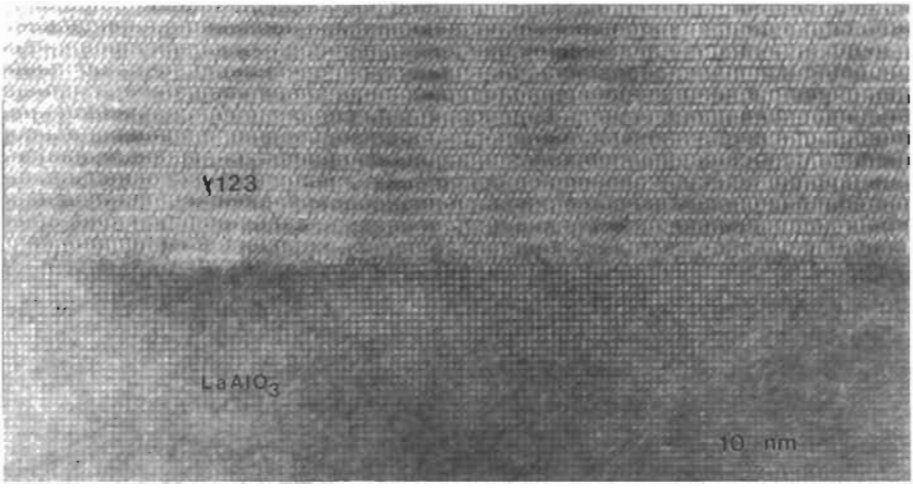

Figure 6 **High-resolution transmission electron microscopy image of an epitaxial thin film of $Y_1Ba_2Cu_3O_{7-x}$ grown on $LaAlO_3$, shown in cross section. (Courtesy of T. E. Mitchell, Los Alamos National Laboratory)**

0.2 nm. Image simulation techniques are necessary to determine the atomic structure of defects imaged by HRTEM.

Specimen Preparation

Probably the most difficult, yet at the same time, most important aspect of the TEM technique is the preparation of high-quality thin foils for observation. This is an old, ever-expanding, complicated, and intricate field of both science and art. There is no simple way to treat this subject briefly. We will merely mention its importance and list some references for further details. It is important to realize (managers, take notice) that the most labor intensive aspect of TEM is the preparation of a useful sample.

In the early days of TEM, sample preparation was divided into two categories, one for thin films and one for bulk materials. Thin-films, particularly metal layers, were often deposited on substrates and later removed by some sort of technique involving dissolution of the substrate. Bulk materials were cut and polished into thin slabs, which were then either electropolished (metals) or ion-milled (ceramics). The latter technique uses a focused ion beam (typically Ar^+) of high-energy, which sputters the surface of the thinned slab. These techniques produce so-called plan-view thin foils.

Today, there is great interest in a complementary specimen geometry for observation, that of the cross section. Cross sections usually are made of layered materi-

als. The specimens are prepared so as to be viewed along the plane of the layers. The techniques for producing high-quality cross sections are difficult, but rather well established. For additional information on sample preparation, consult Thompson-Russell and Edington[8] and the proceedings of two symposia on TEM sample preparation sponsored by the Materials Research Society.[9, 10]

Conclusions

TEM is an established technique for examining the crystal structure and the microstructure of materials. It is used to study all varieties of solid materials: metals, ceramics, semiconductors, polymers, and composites. With the common availability of high-voltage TEM instruments today, a growing emphasis is being placed on atomic resolution imaging. Future trends include the use of ultrahigh vacuum TEM instruments for surface studies and computerized data acquisition for quantitative image analysis.

Related Articles in the Encyclopedia

STEM, SEM, EDS, EELS

References

1 M. von Heimendahl. *Electron Microscopy of Materials: An Introduction.* Materials Science and Technology Series (A. S. Nowick, ed.) Academic, New York, 1980, Chapter 1. This is an excellent introductory guide to the principles of TEM.

2 L. Reimer. *Transmission Electron Microscopy: Physics of Image Formation and Microanalysis.* Springer-Verlag, Berlin, 1984. This is an advanced but comprehensive source on TEM. Reimer also authored a companion volume on SEM.

3 P. B. Hirsch, A. Howie, R. B. Nicholson, D. W. Pashley, and M. J. Whelan. *Electron Microscopy of Thin Crystals.* Butterworth, Washington, 1965, Chapter 4. This sometimes incomprehensible volume is *the* classic textbook in the field of TEM.

4 R. H. Geiss. Introductory Electron Optics. In: *Introduction to Analytical Electron Microscopy.* (J. J. Hren, J. L. Goldstein, and D. C. Joy, eds.) Plenum, New York, 1979, pp. 43–82.

5 J. W. Edington. *Practical Electron Microscopy in Materials.* van Nostrand Reinhold, New York, 1976. This is an excellent general reference and laboratory handbook for the TEM user.

6 B.D. Cullity. *Elements of X-Ray Diffraction.* Addison-Wesley, Reading, 1956. This is a good general reference concerning X-ray diffraction techniques.

7 E. Hecht and A. Zajac. *Optics.* Addison-Wesley, Reading, 1974, Chapter 14. This entire book is an invaluable reference on the principles of optics.

8 K. C. Thompson-Russell and J. W. Edington. *Electron Microscope Specimen Preparation Techniques in Materials Science. Monographs in Practical Electron Microscopy, No. 5.* Philips Technical Library, Eindhoven & Delaware, 1977.

9 *Specimen Preparation for Transmission Electron Microscopy I.* (J. C. Bravman, R. M. Anderson, and M. L. McDonald, eds.) Volume 115 in MRS symposium proceedings series, 1988.

10 *Specimen Preparation for Transmission Electron Microscopy II.* (R. M. Anderson, ed.) Volume 199 in MRS symposium proceedings series, 1990.